CHAPTER III

MORPHOLOGY & PROPERTIES OF BLENDS OF CELLULOSE ESTER AND LIGNIN DERIVATIVES.

CHAPTER III

MORPHOLOGY & PROPERTIES OF BLENDS OF CELLULOSE ESTER AND LIGNIN DERIVATIVES.

ABSTRACT

Commercially available cellulose actetate butyrate (CAB, unplasticized) was blended in melt and solution with lignin esters with different ester substituents - acetate (LA), butyrate (LB), hexanoate (LH) and laurate (LL). LA and LB were compatible with CAB on the 15-30 nm-scale probed by dynamic mechanical thermal analysis and differential scanning calorimetry, and the glass transitions followed the Fox equation. However, broader transitions corresponding to the glass transitions of the two components were observed for CAB and LH and LL blends. This revealed semi-compatibility for CAB/LH and CAB/LL blends. Transmission electron micrographs revealed differences in the phase dimensions of the blends in accordance with chemical and processing (i.e. melt vs. solvent) differences. Modest gains in modulus were observed for low contents (up to 20 wt. %) of LA and LB.

INTRODUCTION

Wood, a natural composite containing carbohydrates and lignin, has been an ideal framework for composite development. In the cell wall of wood, there exists an intimate association between the carbohydrates, the reinforcing component (cellulose) and a network polymer matrix (lignin), which binds the cellulose. This association imparts the strength and rigidity of the wood as is demonstrated in tall trees. Various researchers have tried to emulate this fiber-matrix interface characteristic of wood for achieving better performance in polymer composites. However, the interaction between cellulose and lignin is not well understood.

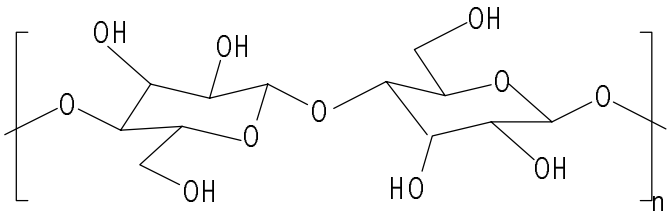

Cellulose

(In case of esters, H is partly or fully replaced by CH_3 for acetate, C_2H_5 for butyrate)

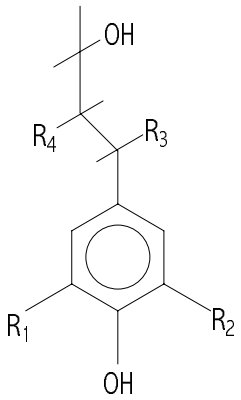

Organosolv Lignin

R_1 mostly OCH_3, H or other unit
R_2 mostly OCH_3
R_3 mostly OH or other unit
R_4 mostly other unit

Studies in the past have demonstrated some compatibility between modified cellulose and modified lignin. Blend studies on melt-extruded and solvent-cast films of hydroxypropyl cellulose (HPC) and lignin (L) revealed the presence of secondary interactions between the two components [Rials and Glasser (1989 b)]. The lignin component was found to reinforce the amorphous cellulose derivative matrix, which forms an oriented crystal mesophase structure, and this behaves as a nano-composite structure. However, this interaction leading to greater miscibility between HPC and L

was not attributed to secondary interactions by hydrogen bonding as reported earlier for other blend systems [Coleman and Painter (1984)]. The effect of hydrogen bonding was studied by partial removal of hydroxy functionality of lignin by ethylation, acetylation, and hydroxy-propylation [Rials (1986)]. Removing the hydroxy functionality from lignin did not influence component miscibility substantially. But the different lignin hydroxy group modifications did influence the blend morphology presumably by altering the conformational stability of lignin (created by a network of intramolecular hydrogen bonds). Further studies were reported on interactions of cellulose derivatives and lignin by modifying the original hydroxy functionality of cellulose [Rials and Glasser (1989 c)]. Cellulose derivatives, such as ethyl cellulose (EC) and cellulose acetate/butyrate (CAB), revealed lower compatibility with lignin showing heterogeneous, two-phase morphology both by differential scanning calorimetry (DSC) and scanning electron miscroscopy (SEM) over a wide range of compositions. The enhanced miscibility of hemicellulose and lignin has been attributed to the introduction of carbonyl functionality by acetylation [Erins et. al. (1976)]. However, this interaction-promoting feature of C=O groups was observed for only a small composition window for CAB and lignin blends (0 to 20% and 80 to 100% lignin content) [Rials and Glasser (1989 c)]. It was also noted that DSC revealed higher compatibility in CAB/L than EC/L blends. Further investigations were carried out by Dave/ and Glasser with the intent of understanding the interaction between liquid crystalline cellulose derivatives and lignin [Dave and Glasser (1997)]. Higher degrees of phase mixing were reported for the continuous fibers prepared from anisotropic solutions of CAB and L in DMAc. Moreover, the addition of lignin to CAB solutions decreased the dynamic viscosity, dynamic elastic modulus and dynamic loss modulus.

Esterification of lignocellulosic materials has been practiced since the early forties for the purpose of improving physical properties. Studies on vapor phase esterification (acetylation) of wood have revealed improvements in the moisture sorption, dimensional stability and biological resistance to high performance wood based composites due to partial reduction of the hydroxyl group content in the lignocellulosic materials [Rowell (1990)]. However, a new technique of preparing blends of cellulose esters and lignin esters has recently been developed by Glasser and Jain [Jain and Glasser (1997)]. This is based on the concept of utilizing the cellulose ester – lignin ester combination as a viable thermoplastic polymer for commercial applications. The novelty of this technique lies in the joint esterification of cellulose and lignin in steam exploded wood (i.e. a mixture of cellulose and lignin) to produce a thermoplastic polymer blend. The separation of the lignin ester component from the cellulose ester component is achieved by appropriate fractional precipitation following the homogeneous esterification reaction of the steam exploded fibers. Also by varying the different solvent to water ratios, cellulose esters containing a desired amount of lignin ester can be precipitated. This promises to eventually reduce the cost of delignification, which conventionally uses severe reaction and separation processes.

This study is based on the understanding of the interactions between a commercial cellulose ester (cellulose acetate butyrate) and lignin esters having different ester group substituent (acetate, butyrate, hexanoate and laurate). Cellulose acetate butyrate has been commercially used for certain specific applications. Modifications with biodegradable additives like lignin may enhance its utilization as well as reduce the cost.

EXPERIMENTAL

MATERIALS

Cellulose acetate butyrate (CAB 381-20), henceforth denoted as CAB, was obtained in powder form from Eastman Chemical Company, Kingsport, Tennessee. The average acetyl and butyryl contents were 13.5 and 38.1 wt.% and the falling-ball viscosity was 20 seconds (76 poise). The number average molecular weight (Mn) was 69,600 with a molecular weight distribution (MWD) of 1.83. Other parameters are detailed in table 3.1.

Lignin acetate (LA), lignin butyrate (LB), lignin hexanoate (LH) and lignin laurate (LL) were prepared by esterification of organosolv lignin (L) as mentioned in chapter II of this thesis. Organosolv Lignin (L) was obtained from Aldrich Chemical Company, WI, USA (Catalog #: 37,101-7). The glass transition temperatures and other specific details are mentioned in Table 3.1.

The powders were dried under vacuum at 40^0C for 12 hours before being blended.

METHODS

Blend Preparation

CAB/lignin ester blends having different proportions of CAB and lignin esters (LA, LB, LH and LL) by weight were prepared by solvent casting and melt extrusion. For preparation of the blends by solvent casting, the blend components were stirred in chloroform (blend concentration of approximately 5% by weight of the solution) at room temperature until all the material was totally dissolved. The solution was then cast in a teflon mold and kept at room temperature in a dessicator for 72 hours so as to evaporate the solvent (chloroform) in a controlled manner. The solvent cast blend was then put in a vacuum oven at 35 ^{0}C for 12 hours to remove any remaining solvent.

For the preparation of blends by melt extrusion, corresponding amounts of individual components were physically mixed at room temperature in a beaker until the color of the mixture looked homogeneous. The mixed powder was then transferred to a preheated "Mini-Max Molder" injection molder from Custom Scientific Instruments. The temperature of the injection molder fixture was maintained at 220^0C. The powder was placed inside the barrel of the molder where it was melted and blended. The polymer was melt-mixed in the molder, with continuous stirring, for approximately two minutes before it was injected into the mold. The injection plunger was manually raised and lowered during this time to improve mixing. The mold cavity was heated through conduction from the fixture and the polymer melt during the injection process and so can be considered as a preheated mold. The cooling rate was not controlled after injection. Consequently, the specimens should be considered to have been quenched.

Two types of specimens were molded: rectangular DMTA specimens and dog bone Minimat specimens. Rectangular specimens had dimensions of 38 mm x 12.6 mm x 1.6 mm. Dog bone specimens, had a nominal length of 38 mm long with a gage section measuring 10.7 mm x 1.7 mm x 3.3 mm.

Differential Scanning Calorimetry (DSC)

The thermal analysis of the samples was determined on a Perkin-Elmer Model DSC-4 equipped with a Thermal Analysis Data Station (TADS) using standard aluminum pans. Measurements were made on ca. 10 mg samples in the temperature range between –20 and 180^{0}C at a scanning rate of 10^{0}C/min. Nitrogen was used as a sweeping gas. The instrument was calibrated with an indium standard. The glass transition temperature was reported from the second heating scan, unless otherwise indicated. The glass transition temperature (T_g) was taken as the temperature at the midpoint (1/2 ΔC_p) of the transition.

Dynamic Mechanical Thermal Analysis (DMTA)

The dynamic mechanical properties of the blend samples were determined in a dynamic mechanical thermal analyzer (DMTA) by Polymer Laboratories Ltd., Shropshire, England. The samples were loaded horizontally in DMTA standard medium size clamps. Measurements were performed in the single and dual cantilever-bending mode for injection molded samples, and in the shear mode for solvent cast films. The shear mode was preferred to bending mode for most of the data as the DMTA showed better transitions in the shear mode. The spectra were collected from -20^{0}C to 180^{0}C using a heating rate of 4^{0}C/min and a frequency of 1.0 Hz. The final temperature of scan varied from sample to sample depending on the onset of melting where the value of tan δ was above allowable limits and the DMTA was out of balance.

Mechanical Properties

The mechanical properties (modulus, strength and ultimate strain) of the blends were determined on a Miniature Materials Tester (Minimat model # SM9-06) by Polymer Laboratories, Loughborough, England. Tests were conducted at room temperature with a 1000 N load beam using strain rates of 5 mm/min. The calculation of modulus and strength were based on the initial cross sectional area. The reported data represents the average of four measurements for each composition.

Transmission Electron Microscopy (TEM)

Samples were embedded in Poly/Bed 812 (Polysciences, Inc.) cured at 60^{0}C for 48 hours in flat molds. 80-100 nm thick sections were cut from the embedded films with a diamond knife mounted on a Reichert Ultracut E microtome. The sections were carefully mounted on copper grids. The grids were observed on a JEOL JEM-100CX-II electron microscope operated at an accelerating voltage of 80 kV. The micrographs were from the bright field images of the cut unstained samples at a magnification of 10,000x.

Rheological Characterization

Rheological measurements were performed to determine the complex viscosity (η^*) of the CAB/LA blends in a Rheometrics RMS-800 rheometer using 25 mm parallel plates as tooling. The experiments were run in dynamic mode with a maximum of 15% strain. The maximum strain was determined for the samples by a strain sweep experiment at 200^{0}C and obtaining the linear viscoelastic region for the polymer as shown in Fig. 3.1. Sample preparation involved the mechanical mixing of the dry powders of the two

components at room temperature and then fusion of the mixture in a circular mold of approximately 2.54 mm in diameter at elevated temperatures (180-200^{0}C). The samples were dried in a vacuum oven (pressure = 1.0 mm of Hg) for at least 24 hours before testing to remove any moisture from the samples. The experiments were conducted in a nitrogen atmosphere. The temperature was held constant for 3 minutes before starting the test to ensure thermal equilibrium between the tooling and the sample.

RESULTS

THERMAL ANALYSIS

- **DSC Results**

The results obtained from DSC reveal single glass transition temperatures (T_g's) for all CAB/LA blends (Fig. 3.2 and Table 3.2). The T_g's shift towards the glass transition of LA as LA content increases in the blends. The values follow the Fox equation [Fox (1956)] (Fig.3.3). Similar results are obtained for CAB/LB blends (Figs. 3.4) and the glass transition temperatures of the blends can be represented by the Fox equation (Fig. 3.3). However, in all the above cases the transitions become broader for blend compositions of 70/30 to 30/70 of CAB/LA or CAB/LB due to the convolution effects from both components.

For CAB/LH blends, distinct second order transitions corresponding to the two components were observed in the first heating scans of DSC (Fig. 3.5). The lower transition corresponds to the glass transition of LH, whereas the transition at the higher temperature is from the CAB component. It is also observed that the transitions occur almost in the same regions as those of the individual pure components, and they do not shift much with variation in the compositions of the blends. However, the transition corresponding to the CAB component becomes weaker as the amount of LH increases in the blend and this transition ultimately remains undetected at a composition of 50% CAB. This might be due to dilution of the transition of CAB as compared to that of LH at high LH content in the blend.

However, in the second heating scans, only one transition is observed for each blend composition (Fig. 3.6). This single transition is broader and it is not clearly distinguishable for LH contents higher than 20 weight % in the blends. This disappearance of T_g-transitions in lignin during repeated heating has been noted before and it suggests some sort of reorganization in the rubbery state. No additional explanation can be given. This behavior is expected to be similar to that observed for melt blended samples and the DSC for melt blended samples of CAB/LH reveal a similar pattern in the glass transition behavior (Fig. 3.7). However, in case of CAB/LH blends, the glass transition temperatures of the blends do not follow the Fox equation (Fig. 3.8). DSC results for CAB/LL blends were similar to those of CAB/LH blends and the glass transition temperatures do not obey Fox equation (Fig. 3.9).

- **DMTA Results**

Dynamic mechanical measurements of CAB/LA blends reveal a shift in the modulus curves (E' and E'') towards lower temperatures as the amount of LA increases in the blends (Figs. 3.10 and 3.11). Similarly, the tan δ peaks also shift towards lower temperatures as LA content increases (Fig. 3.12). However, all compositions of the CAB/LA blends are represented by single tan δ and E'' curves representing single glass transitions of the blends. The glass transition temperatures obtained from the points of inflexion (where the derivative of the slope of the curve is zero) of the loss modulus curves correspond to those obtained from DSC results and they follow the Fox equation (Fig.3.3). Again, the tan δ peaks broaden as the LA content increases due to the convolution effects of the glass transitions of both components.

Similarly, for CAB/LB blends, all compositions are described by modulus shifts towards lower temperatures as well as by single tan δ and loss moduli (E'') peaks (Figs. 3.13, 3.14, 3.15). The discontinuities in the modulus curves are attributed to volume changes that take place near the glass transition temperature of lignin. This causes the dynamic mechanical analyzer to go out of balance when the experiments are performed in bending mode. This can be avoided by performing the experiments in the shear mode as can be seen for lignin hexanoate blends discussed later. The glass transitions represented by the points of inflexion of the loss modulus curves are comparable to the glass transition temperatures obtained from DSC results and they follow the Fox equation (Fig.3.3). However, the decrease in the storage modulus (E') curves occurs over a wider temperature range as the LB content increases in the blend. The modulus flattens out to greater extent with increasing LB content after decreasing by 2 decades in value (Fig. 3.13). This behavior is pronounced only in the case of CAB/LB blends and not for the other blends. It is somewhat similar to the behavior found in the cold crystallization of polymers where the modulus is retained even after the glass transition temperature, possibly due to the re-orientation of the polymer chains above their glass transition. Therefore, the LB component might be the factor in bringing in some sort of molecular reorganization in CAB, which can retain the modulus over a wider temperature range. The effect of lignin (derivatives) on the organizational behavior of cellulose derivatives has been noted before [Rials and Glasser (1989c); Dave and Glasser (1997)].

In case of CAB/LH blends, however, an emergence of a second peak corresponding to the LH component is observed in the loss modulus curves obtained by DMTA analysis in the bending mode (Fig. 3.16). The peaks gradually separate out as the amount of LH is increased. However, the tan δ peaks reveal single transitions which shift towards lower temperatures except in the case of the highest LH content where a shoulder is found near 80^0C (Fig. 3.17). This might be due to lower resolution of the effect of the glass transition of the LH phase as compared to the CAB phase, and only the transition of the CAB phase is prominent at lower LH content. It is also observed that the points of inflexion of the loss modulus curves of the CAB/LH blends corresponding to the CAB component are shifted from their original peak for pure CAB (Fig. 3.16). However, in case of the DMTA results for solvent cast films of CAB/LH in the shear mode, the emergence of a lower temperature transition is observed as the amount of LH increases in the blend (Figs. 3.19, 3.20, 3.21). The transitions, as shown by the loss modulus curves, reveal broad transitions over a wide temperature range for high LH contents in the blends. Similar results were obtained for CAB/LL blends (Figs. 3.22, 3.23, 3.24).

TRANSMISSION ELECTRON MICROSCOPY (TEM) RESULTS

Transmission electron micrographs of solvent cast blends of CAB with 20 and 50 wt. % of LH clearly indicate differences in the size of the LH phases dispersed within the continuous CAB phase (Fig. 3.25). The darker phase represents the lignin component due to the higher electron density (i.e., presence of conjugated π electrons in the phenyl rings) of lignin molecule. Comparison between solvent cast and melt blended samples of 20%LH/CAB reveals greater dispersion of the LH phase when melt blended compared to solvent cast (Fig. 3.26). The mean domain sizes (obtained by averaging the domain sizes of the lignin ester phases within a square inch cross-sectional area of the TEM micrographs) of CAB/LH blends for solvent casting is 1000 nm as compared to 170 nm for melt blended samples. Solvent casting can be considered to be an equilibrium process. Therefore, the lignin ester molecules tend to aggregate together (as in case of an immiscible solution) to obtain the lowest possible energy configuration and form larger domains. In case of melt blending, the external shear force applied as well as high rate of subsequent cooling from melt is a non-equilibrium process which leads to greater dispersion of the lignin ester molecules in the CAB phase. Hence the domain sizes of the lignin ester phases are smaller in case of melt blending as compared to solvent casting. This is a kinetically controlled as opposed to thermodynamically controlled process.

A comparison between the blends of CAB/LA and CAB/LH containing the same percentage of lignin ester (20 wt. %) reveals a significant differences in the domain sizes of the lignin ester phases (Fig. 3.27). The domain sizes for melt processed CAB/LA blends vary between 10-100 nm whereas they are 75-500 nm for CAB/LH blends.

MECHANICAL PROPERTIES

Lignin is a small molecule ($M_n < 1000$) as compared to the high molecular weight CAB ($M_n \approx 70{,}000$). Also it has been found from the transmission electron micrographs that the lignin phase is dispersed in the CAB continuous phase. Therefore, this combination acts as a nano-composite with the lignin component acting as the reinforcing filler for the CAB phase. Lignin, being a small glassy molecule at room temperature, enhances the modulus of the continuous phase. This effect is revealed by the mechanical property analysis of the blends at room temperature.

The mechanical properties (tensile strength, strain at break and modulus) of the CAB/lignin ester blends are presented in Figs. 3.28, 3.29, 3.30. In case of CAB/LA blends, a 10% increase in the modulus is obtained for 10% incorporation of LA in CAB. However, the modulus henceforth decreases at LA contents > 10 wt. % possibly due to inadequate stress transfer between the phases as seen by a drastic decline in the ultimate strain. The tensile strength, however, decreases with addition of LA due to decreased stress transfer between the CAB and LA phases.

Similar results are observed for CAB/LB blends (Fig. 3.29). However, the modulus increases more than 20 % with LB content rising to 20 wt.%. A possible molecular reorganization and its effect on the modulus of CAB/LB blends had been discussed earlier. It is more probable that the interaction of LB with CAB is more pronounced than LA with CAB because of higher butyryl than acetyl content in CAB. However, the tensile strength and ultimate strength decrease due to poor stress transfer

between phases. Therefore, LB is a better modulus builder in CAB than LA and the optimum lies around 20 wt. % LB.

In case of CAB/LH blends, the modulus does not increase and remains almost equal to that of native CAB up to 20 wt. % of LH loading (Fig. 3.30). However, in case of LL a decrease in modulus is observed (Fig.3.30). In all the blend samples of CAB/lignin ester blends, the maximum strain (i.e. strain at break) and tensile stress decrease with the addition of lignin esters. This reflects poor stress transfer between phases due to the glassy nature of the lignin esters. However, in case of LL blends, the strain at break values levels off at a value near 7% (Fig.3.29). This is due to LL (which has a T_g lower than room temperature) and therefore LL phase is a rubbery phase at room temperature, at which the tensile experiments are carried out. Hence, stress transfer is possible between the rubbery LL phases and the continuous CAB phase revealing better strains at break for high lignin ester contents than LA, LB or LH blends.

RHEOLOGICAL CHARACTERIZATION

Melt viscosity measurements were carried out at three different temperatures (200^0, 220^0 and 240^0 C). The data are plotted in terms of the complex viscosity (η^*) vs. frequency (ω) for LA contents of 0, 10 and 20 wt % in the blend (Figs. 3.31, 3.32, 3.33). The viscosity of the CAB/LA blends was found to be greater than the viscosity of pure CAB at all temperatures of measurement. However, the relative amount of LA content in the blend had no influence on the absolute value of the complex viscosity and so the viscosity curves for 10% and 20% LA contents were essentially overlapping each other. This behavior of increase in viscosity has been reported earlier for polypropylene-lignin blend systems [Kosikova et.al. (1993)]. The decrease in the shear stress (i.e., increased viscosity) at constant shear rates for polypropylene-lignin blends have been attributed to the possibility of increased crosslinking between the two components. However, in case of CAB/LA blends, LA acts as a plasticizer for CAB and reduces the glass transition temperature of the blend system. Also crosslinking between CAB and LA is not probable since most of the hydroxyl groups of lignin have been replaced by ester substituents. There has been no evidence to suggest that lignin undergoes cross-linking or trans-esterification with CAB. Therefore, the reason for the increase in viscosity when lignin component is added cannot be explained at this stage as this contradicts the behavior of a plasticizer. Another possible reason might be the inadequate dispersion of LA into CAB phase. The samples for the test were prepared by fusion of the polymer particles, and no adequate dispersion was achieved during the test, since the tests were run at a maximum strain of 5-15% to minimize the effect of lubrication by LA. Therefore, the individual polymer phases present within the sample may have been much greater than that required for LA to act as a polymeric plasticizer. Further studies are needed to substantiate the above plasticizing and rheological effect of LA on CAB.

DISCUSSIONS

Before discussing any of the results of the CAB and lignin ester blends, the term "compatibility" related to polymer blends should be described here. The term compatibility has been used extensively in case of polymer blends to define the interaction between polymer pairs at the molecular level. However, when it comes to macromolecules or polymers, the dimensions of the molecules can vary by a large extent and the term "molecular level" has no clear significance. Therefore, the compatibility or homogeneity of a polymer blend can only be defined in relative terms of dimensions of the separate phases which can be generally characterized by different measurement techniques such as Differential Scanning Calorimetry (DSC), Dynamic Mechanical Spectra (DMS), Thermo-Mechanical Analysis (TMA), Nuclear Magnetic Resonance Spectra (NMR) etc.

Hence, compatibility is treated as a relative term and can be defined by a compatibility number, [Kaplan, 1976]

$$N_c = \frac{\text{Experimental Probe Size}}{\text{Domain Sizes of Phases}}$$

The experimental probe size can be taken as the scale of resolution of an instrumental technique. The domain size is the average dimension of each existing phase in the polymer blend.

Thus, i) when $N_c \longrightarrow \infty$, the system is compatible
ii) when $N_c \longrightarrow 1$, the system is semicompatible
iii) when $N_c \longrightarrow 0$, the system is incompatible

When N_c approaches zero, the dimension of each existing phase is much greater than the probe size of the instrument and so the instrument can detect two separate transitions corresponding to each phase component. Here two distinct T_g 's are observed.

For the compatible case (i.e., N_c approaches ∞), the probe size is much greater than the phase dimensions and so the instrument is unable to detect small compositional fluctuations and so report a single T_g which is an average of the contributions of each component.

For the semicompatible case, a broader effect of the corresponding transitions is observed and a great deal of damping over the entire temperature range from the lower to the higher transitions associated with each component.

Therefore, the detection of a single or double transition in a two phase system by an instrument gives an indication of the dimensions of the phases present in the system. The dimension that corresponds to a dynamic mechanical thermal analysis is approximately 15-30 nm [Kaplan, 1976]. NMR technique on the other hand can detect composition fluctuations in the dimensional range of 2.5-5 nm [Masson and Manley, 1992].

The results observed from the DSC and DMTA results for CAB/LA and CAB/LB show single glass transitions for all the blend compositions and the T_g's follow the Fox equation. This predicts some interaction between the CAB and LA (or LB) components and hence compatibility of the two components in the 30-150 nm scale as explained

earlier. The TEM results also proved that the phase dimensions are in the range of 10-100 nm for melt blended samples of CAB/LA. Therefore, LA and LB acts as a polymeric plasticizer for CAB and effectively reduces the glass transition temperature of the blends.

However, when CAB is blended with LH or LL, two distinct glass transitions are observed by both DSC (in first heating scans) and DMTA. This reveals that the phases of CAB and LH (or LL) are large enough (greater than 150 nm) to produce two separate transitions corresponding to the two components (CAB and LH or LL) of the blends. CAB contains both acetyl and butyryl groups and interactions between the similar groups in lignin esters and CAB are expected. The ester substituent (hexanoate) in case of LH is much bigger in size compared to acetate and butyrate and interaction between the CAB and LH is less pronounced. This leads to greater phase separation in CAB and LH and the domain sizes are large enough to reveal two distinct glass transitions. This behavior is also evident from the TEM 's for CAB/LH melt-processed samples, where the phase dimensions are in the range of 75-500 nm (Fig. 3.27). CAB is less compatible with lignin hexanoate and lignin laurate than that with lignin acetate and lignin butyrate. As the ester substituent size increases from two C-atoms (in acetate) to six C-atoms (as in hexanoate), the lignin ester tends to segregate from the CAB and form individually larger phases. Therefore, as the length of the ester substituent in lignin esters increases, the CAB/lignin ester blends proceed from total compatibility to semi-compatibility. The mechanical property measurements also show similar results for the CAB/lignin ester blends. Around 10% modulus increase is observed for both LA and LB blends (which are compatible) at lower lignin ester contents, whereas no increase can be observed in the modulus for LH and LL blends (Fig 3.30). This can be explained from the existing phase dimensions of the lignin ester in the continuous CAB phase. LA and LB are more finely dispersed and help in reinforcing the CAB matrix. But this is not possible in case of LH or LL blends since the reinforcing effect is lost due to lower dispersion leading to larger phase dimensions.

However, the relaxations obtained by the tan δ peaks (or the points of inflexion of the E'' or G'' curves), corresponding to the glass transitions of the CAB and LH (or LL) components, shift on the temperature axis (towards lower temperatures for CAB and higher for LH or LL) with concentration changes in the blend (Figs. 3.8 and 3.9). This shifting of the tan δ towards lower temperatures reveals some interaction between the LH (or LL) and the CAB components. Hence, there is some compatibility between the CAB and LH components although the two blend components phase separate to greater extent than CAB/LA and CAB/LB blends. Though the glass transition temperatures do not follow the Fox equation in case of CAB/LH or CAB/LL blends, the lignin component (LH and LL) plasticizes CAB by depressing the glass transition temperature.

A comparison can be obtained between the separation between the observed glass transitions of the CAB and lignin esters probed by DMTA and the corresponding dimensions of the existing phases in the blends. Figure 3.34 reveals such a relationship where the separation of the glass transitions is zero (or there exists only one transition) for CAB/LA blends when the phase dimension is below approximately 30 nm [Kaplan (1976)]. However, the separation of the T_g's increases gradually as the phase dimension increases because there exists some interaction between the CAB and lignin ester component and the glass transitions are eventually affected to certain extent. Otherwise, if there had been no interaction between the components (i.e. for incompatible blends) the

separation of the transitions would reach its maximum value abruptly once the 30nm dimension size is exceeded.

A comparison can be also drawn for the glass transition relaxations for CAB/lignin ester blends as obtained by different measurement techniques. The nature of the transitions obtained by DSC and DMTA (by E', E", G" and tan δ) have been correlated with the phase dimensions obtained from the transmission electron micrographs in Table 3.3. It is observed that the loss modulus (E") in the bending mode produces two transitions in the 75-500 nm dimension range and is the most sensitive tool to obtain blend properties. However, the loss modulus (G") in the shear mode has been found to produce broad transitions in the above mentioned dimension range. Shear mode is preferred over the bending mode as it can be used very effectively to determine transitions for larger phase separated blends (greater than 500 nm), whereas the bending mode was not, because of the thermal expansion effects near the glass transitions which resulted in discontinuities in the modulus curves. DSC is less sensitive than DMTA in case of CAB/lignin ester blends though two transitions are observed in the first heating curve for greater phase separated blends.

CONCLUSION

The blends of CAB/LA and CAB/LB reveal single glass transitions for all the compositions considered in the study probed by both DSC and DMTA. The transitions follow the Fox equation and hence are compatible on the 30-150 nm scale probed by dynamic mechanical measurements and differential scanning calorimetry. But, in case of CAB/LH and CAB/LL blends, two distinct transitions (or broader transitions) are observed corresponding to the glass transitions of CAB and LH or LL components. TEM results revealed phase dimensions of the lignin ester phases, which were in accordance to the results interpreted from other measurements. Therefore, a transition from full compatibility to semi-compatibility is observed for the CAB/lignin esters blends as the ester chain substituent increases from two to twelve. However, in all the blends, the glass transition temperatures decrease with the incorporation of any of the lignin esters and the lignin esters act as polymeric plasticizers for CAB. The phase dimensions (from TEM results) for solvent cast blends were much greater than those for melt blended samples. Enhancement in the modulus is observed in cases of CAB blends with LA and LB but not for CAB/LH or CAB/LL blends, though the tensile strength and ultimate strain decrease due to lower stress transfer between the components. The enhancement in modulus is due to the low molecular weight glassy lignin ester, which acts as a reinforcing filler in the continuous CAB matrix. However, in contradiction to the properties of a plasticizer, the complex viscosity of CAB increases with the addition of LA. Therefore, the short-chain lignin esters (acetate and butyrate) can be used as a polymeric plasticizer as well as a modulus builder for commercial CAB.

FUTURE WORK

Recommendations for future work include :

1) More detailed study of the blend properties with different ratios of lignin esters for optimization considering specific applications of the blends, such as in composite matrix, moldings etc.
2) Further rheological studies of the CAB/LA blends in order to understand the melt viscosity characteristics of the CAB/LA blends. In this study, the samples for rheological studies were prepared by fusion of the polymer particles at a temperature above 200^0C. Therefore, no dispersion was achieved within the two polymer components. For future rheological studies, the samples can be prepared by melt mixing with dispersion so as to reveal the plasticizing effect of lignin component.

REFERENCES

Ciemniecki, S. L. and Glasser, W. G. (1988), Multiphase materials with lignin: 1. Blends of hydroxypropyl lignin with poly(methyl methacrylate), *Polymer*, Vol. 29, 1021-1029.

Ciemniecki, S. L. and Glasser, W. G. (1989), in *Lignin - Properties and Materials*, Series 397, W.G.Glasser and S. Sarkanen (eds.), American Chemical Society, Washington, DC, 452-463.

Coleman, M. M, and Painter, P. C. (1984), Fourier transform infrared spectroscopy: Probing the structure of muticomponent polymer blends, *Appl. Spec. Revs*., 20(3), 255-346.

Dave, V., and Glasser, W. G. (1992), in *Viscoelasticity of Biomaterials*, Series 489, W.G. Glasser and H. Hatakeyama (eds.), American Chemical Society, Washington, DC, pp. 144-166.

Dave, V.; Glasser, W. G., and Wilkes, G. L. (1992), Evidence for Cholesteric Morphology in Films of Cellulose Acetate Butyrate by Transmission Electron Microscopy, *Polymer Bulletin*, 29, 565-570.

Dave, V. and Glasser, W. G. (1997), Cellulose-based fibers from liquid crystalline solutions: 5. Processing and morphology of CAB blends with lignin, *Polymer*, Vol. 38, 9, 2121-2126.

Erins, P.; Cinite, V.; Jakobsons, M. and Gravitis, J. (1976), Wood as a multicomponent crosslinked polymer system, *Journal of Applied Polymer Science, Applied Polymer Symposium*, 28(2), 1117-1138.

Glasser, W. G., and Jain, R. K. (1993), Lignin Derivatives, *Holzforschung*, Vol. 47 (3), 225-233.

Jain, R. K. and Glasser, W. G. (1997), "Thermoplastic powders from steam exploded fibers by heterogeneous esterification", Patent filed in December, 1997.

Kaplan, D. S. (1976), Structure-Property Relationships in Copolymers to Composites: Molecular Interpretations of the Glass Transition Phenomenon, Journal of Applied Polymer Science, Vol 20, 2615-2629.

Kosikova, B.; Demianova, V. and Kacurakova, M. (1993), "Sulfur-Free Lignins as Composites of Polypropylene Films," *Journal of Applied Polymer Science*, Vol. 47, 1065-1073.

Masson, J. F. and Manley, R. St. John (1992), "Solid-State NMR of Some Cellulose/Synthetic Polymer Blends," *Macromolecules*, 25, 589-592.

Nishio, Y; Matsuda, K; Miyashita, Y; Kimura, N and Suzuki, H; (1997) Blends of Poly (ε–caprolactone) with Cellulose alkyl esters : Effect of the alkyl side-chain length and degree of substitution on miscibility. *Cellulose*, 4, 131-145

Oliveira , Willer de, and Glasser, W.G.(1994) Multiphase materials with Lignin XII. Blends of Poly(vinyl Chloride) with Lignin-Caprolactone Copolymers, *Journal of Applied Polymer Science*, Vol.51, 563-571

Rials, T. G. (1986), Secondary interactions in blends of lignin and cellulose derivatives:

Composite morphology and properties. pages 99-127, Ph.D. Thesis, Virginia Polytechnic Institute and State University, Blacksburg, VA.

Rials, T. G., and Glasser, W. G. (1989a), in *Lignin - Properties and Materials*, Series 397, W. G. Glasser and S. Sarkanen (eds.), American Chemical Society, Washington, DC, pp. 464-475.

Rials, T. G., and Glasser, W. G. (1989b), "Multiphase Materials with Lignin. IV. Blends of Hydroxypropyl Cellulose with Lignin," *Journal of Applied Polymer Science*, Vol. 37, 2399-2415.

Rials, T. G., and Glasser, W. G. (1989c), "Multiphase Materials with Lignin VI. Effect of Cellulose Derivative Structure on Blend Morphology with Lignin," *Wood and Fiber Science*, 21(1), 80-90.

Rowell, R. M. (1990), "Chemical modification of Lignocellulosic Fibers to Produce High-Performance Composites", in *Agricultural and Synthetic Polymers: Biodegradability and Utilization*, Glass, J. E. and Swift, G., Eds. American Chemical Society Press, Washington, DC, 1990, Chapter 21, 242-256.

Fox, T. G., *Bull. Am. Phys. Soc.*, 2 (2), 123 (1956).

Table 3.1 : Molecular weights and glass transition temperature values.

	M_n	M_w	MWD	Mark Houwink Values		T_g (^oC)
				a	Log K	
CAB 381-20	69,600	127,600	1.83	0.788	-3.808	134
Lignin Acetate	1,550	5,890	3.80	0.204	-2.536	92
Lignin Butyrate	2,310	7,730	3.34	0.218	-2.591	52
Lignin Hexanoate	2,650	9,440	3.56	0.222	-2.585	30
Lignin Laurate	13,400	33,200	2.48	0.269	-3.207	2

Table 3.2 : Comparison of glass transition temperatures obtained from DSC analysis and DMTA .

Blend Type	T_g (^{0}C) by DSC [1]	DMTA [2]
CAB 381 – Lignin Acetate		
100/0	136	144
90/10	131	139
80/20	-	136
70/30	120	129
50/50	110	127
30/70	111	-
0/100	92	-
CAB 381 – Lignin Butyrate		
100/0	136	144
90/10	128	138
80/20	121	129
70/30	110	122
50/50	89	-
30/70	73	-
0/100	52	-
CAB 381 – Lignin Hexanoate		
100/0	136	144
90/10	122	136
80/20	121	-
70/30	109	-
50/50	-	-
0/100	30	-
CAB 381 – Lignin Laurate		
100/0	136	144
80/20	125	-
70/30	124	-
50/50	116	-
0/100	2	-

[1] Taken from the second heating scan.
[2] Taken from the maximum of the peak in the tan δ curve.

Table 3.3 : Comparison of glass transition relaxations for CAB/lignin ester blends obtained by various instrumental techniques.

Parameter	**Phase Dimensions (nm)**		
TEM	10-100 [1]	75-500 [2]	500-1000 [3]
DSC	single Tg [4]	broad Tg [5]	two Tg's [6]
E'	single step-transition [7]	two step-transitions [8]	two step-transitions [9]
E'' (bending mode)	single peak [10]	two peaks [11]	_____
G'' (shear mode)	single peak [12]	broad transition [13]	broad transition [14]
tan δ	single peak [15]	broader peak [16]	single broader peak with a shoulder [17]
Mechanical properties	Good [18] (higher modulus)	Moderate [19] (no increase in modulus)	Poor [20] (low modulus)

The referring figures are as follows : [1] Fig.3.27b, [2] Fig.3.27a, [3] Fig. 3.26a, [4] Fig.3.2, [5] Fig.3.7, [6] Fig.3.5, [7] Fig.3.10, [8] Fig. 3.18, [9] not shown, [10] Fig.3.11, [11] Fig.3.16, [12] not shown, [13] not shown, [14] Fig.3.21, [15] Fig.3.12, [16] Fig.3.17, [17] Fig.3.20, [18] Fig.3.30, [19] Fig.3.30, [20] 3.30.

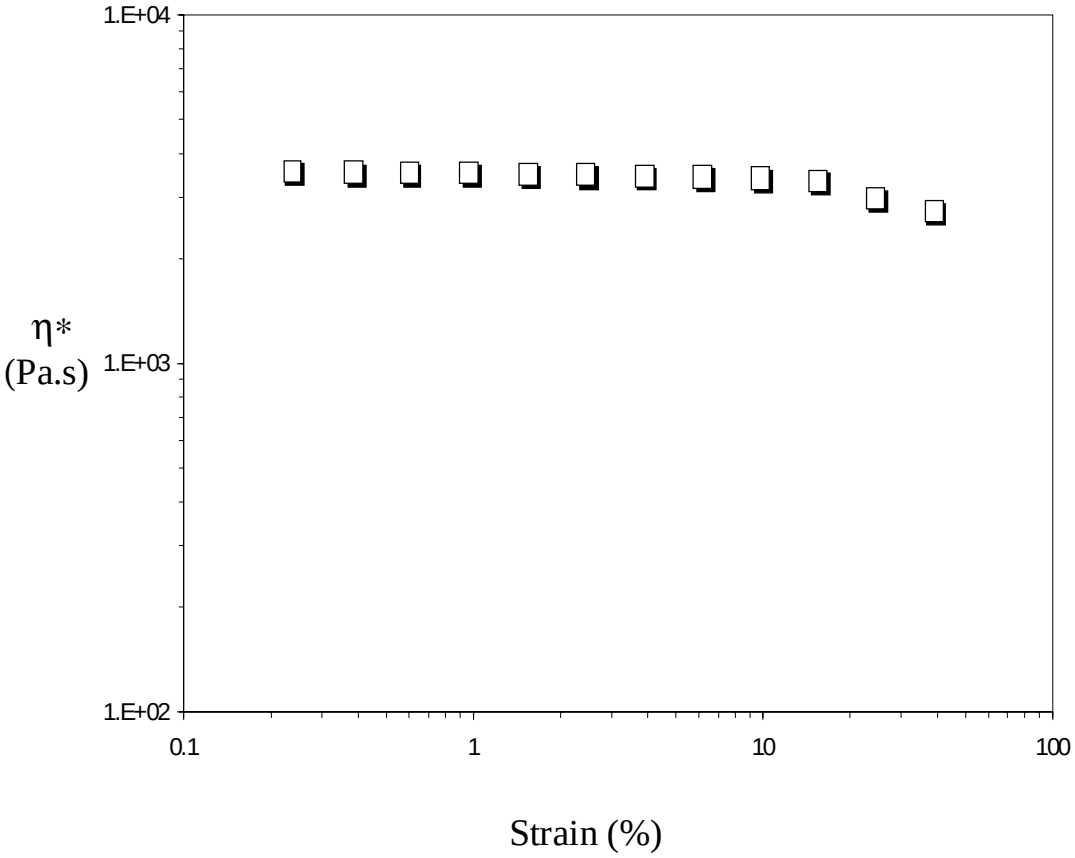

Fig. 3.1 : Strain sweep for pure CAB at 200 ^{0}C for determining the linear viscoelastic region for the polymer.

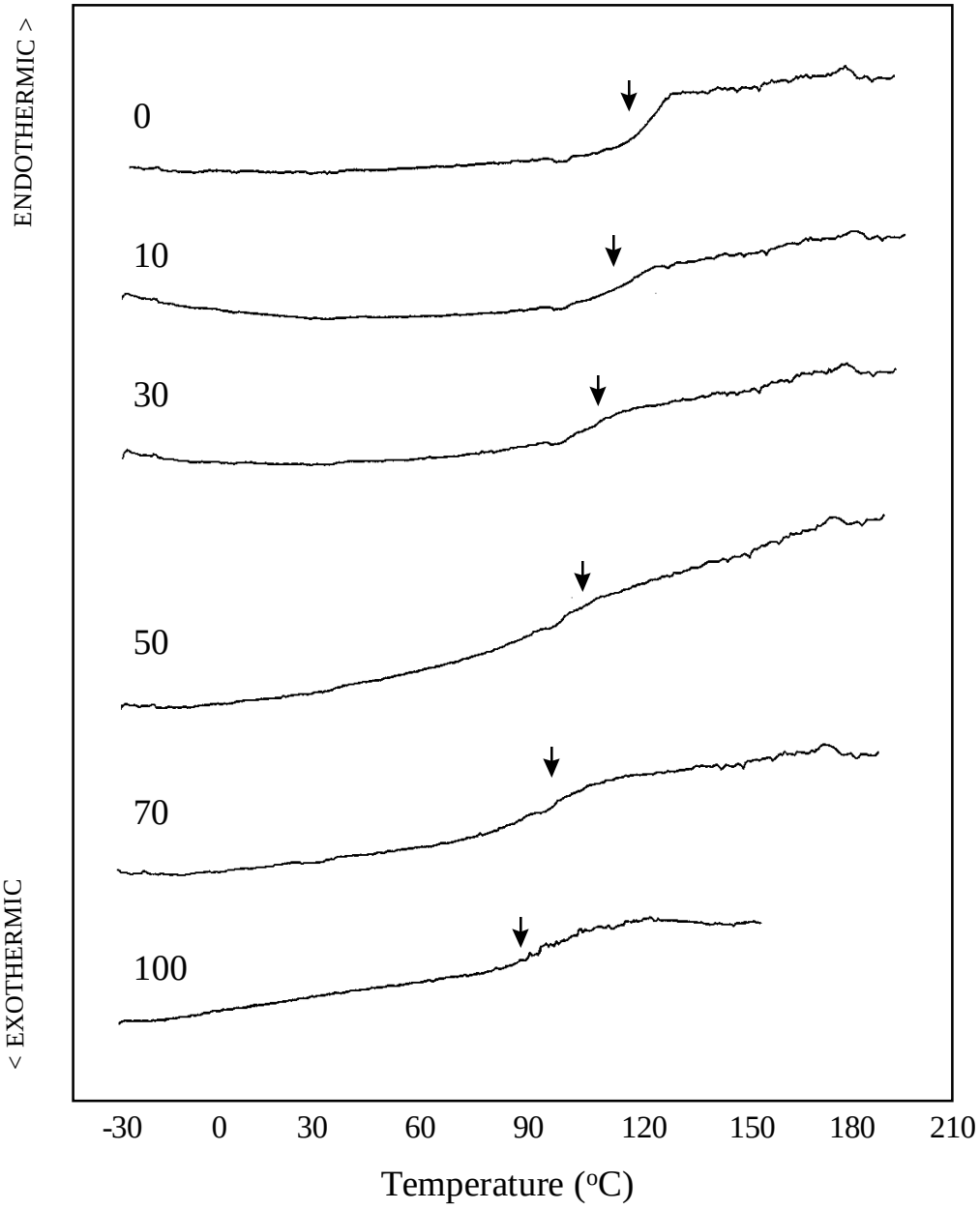

Figure 3.2 : DSC thermograms of solvent ($CHCl_3$) cast samples of CAB and LA. Numbers on each curve denote LA content (wt.%) in the blend. These traces are from the second heating scan (after quenching from melt at a rate of 300 °C/min).

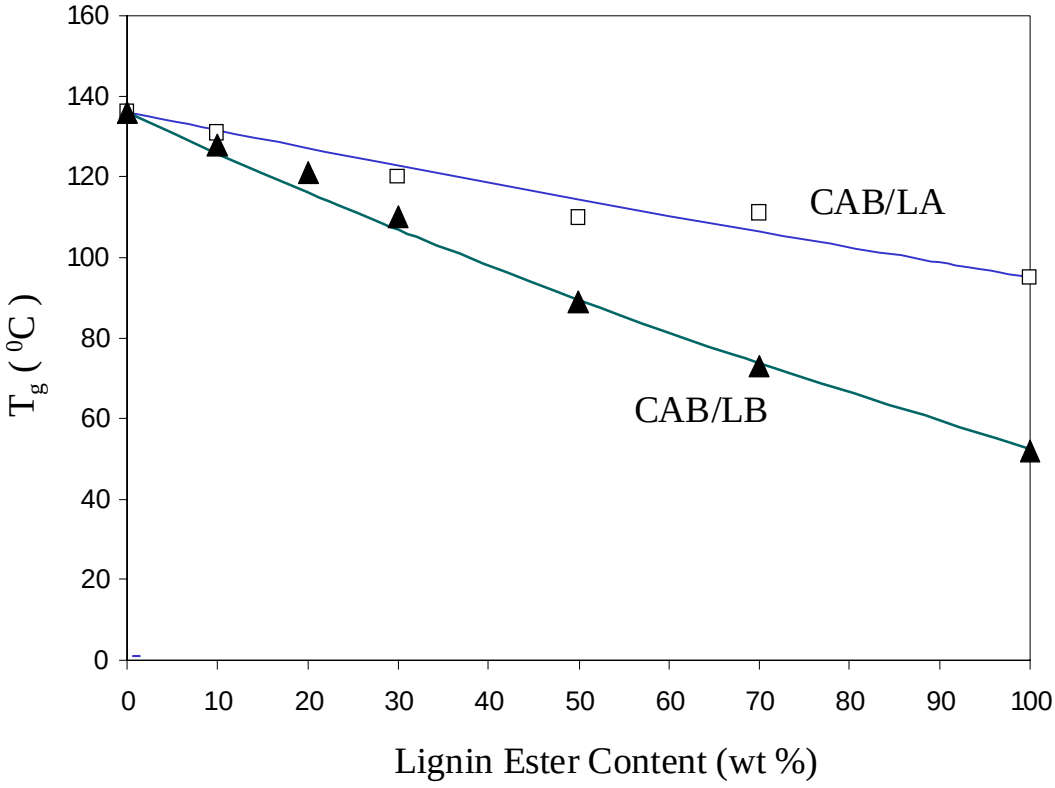

Figure 3.3 : Fox equation fit for blends of CAB and LA or LB. T_g data obtained from DSC scans.

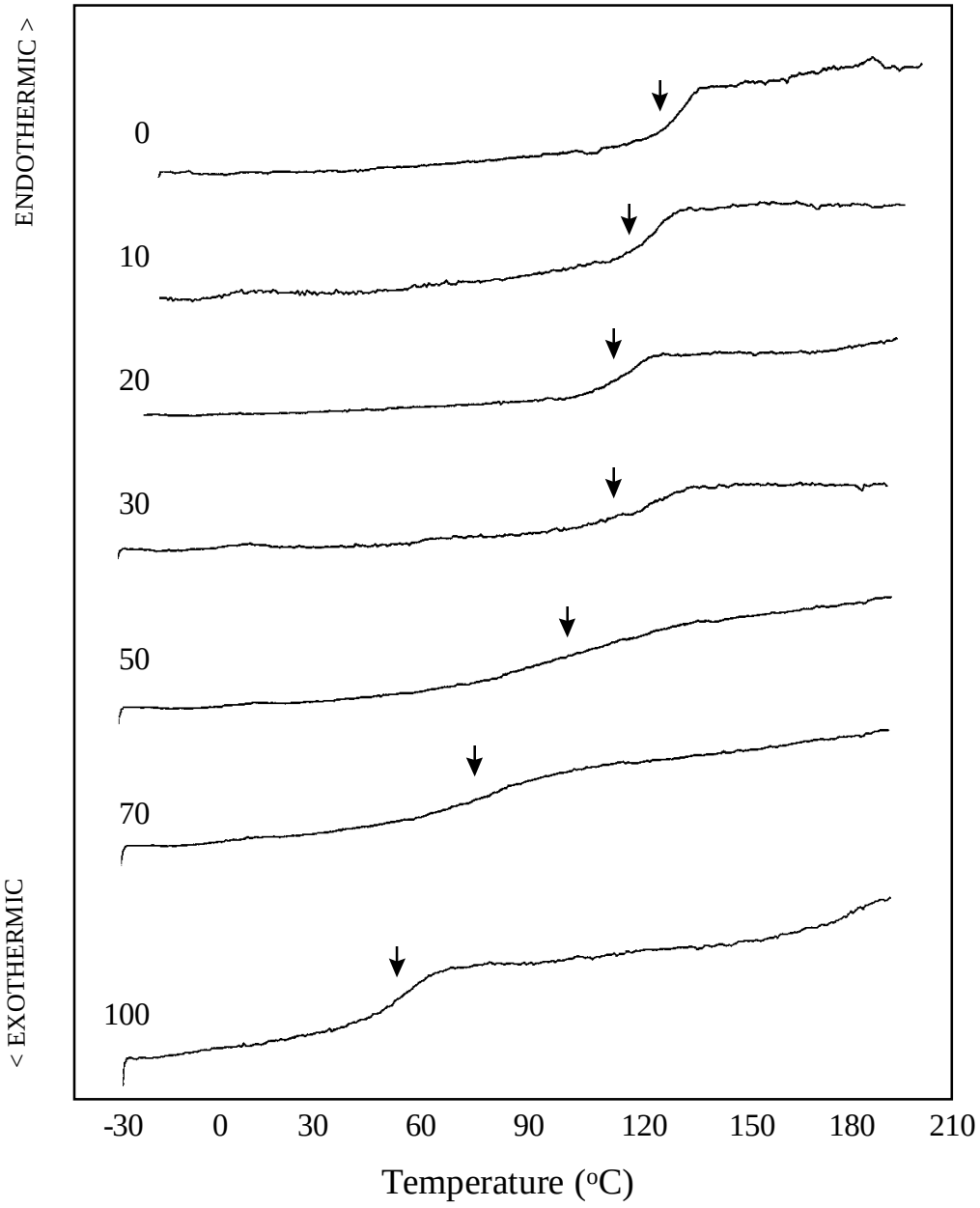

Figure 3.4 : DSC thermograms of solvent ($CHCl_3$) cast samples of CAB and Lignin Butyrate (LB). Numbers on each curve denote LB content (wt.%) in the blend. These traces are from the second heating scan (after quenching from melt at a rate of 300 °C/min).

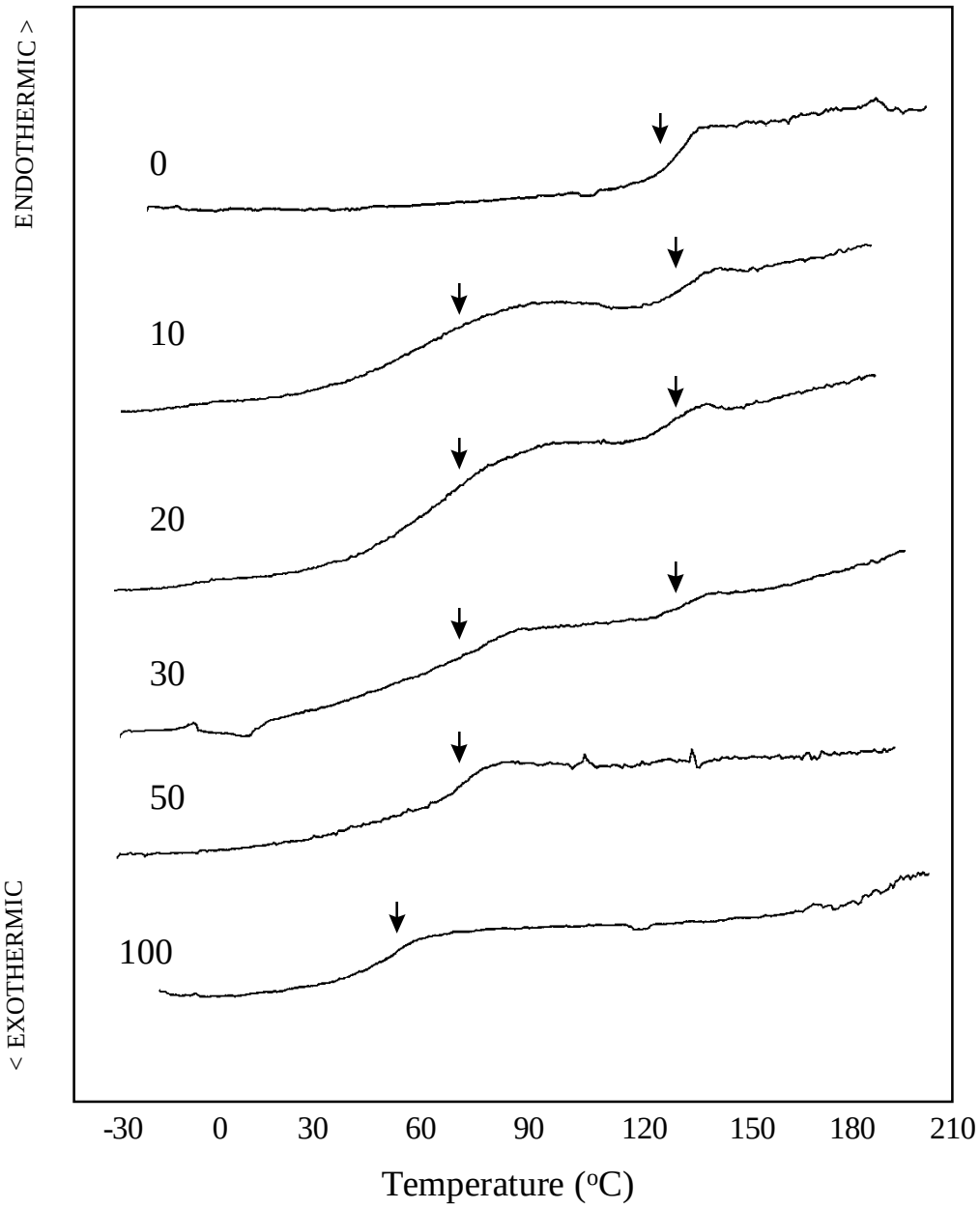

Figure 3.5 : DSC thermograms of solvent ($CHCl_3$) cast samples of CAB and Lignin Hexanoate (LH). Numbers on each curve denote LH content (wt.%) in the blend. These traces are from the first heating scan.

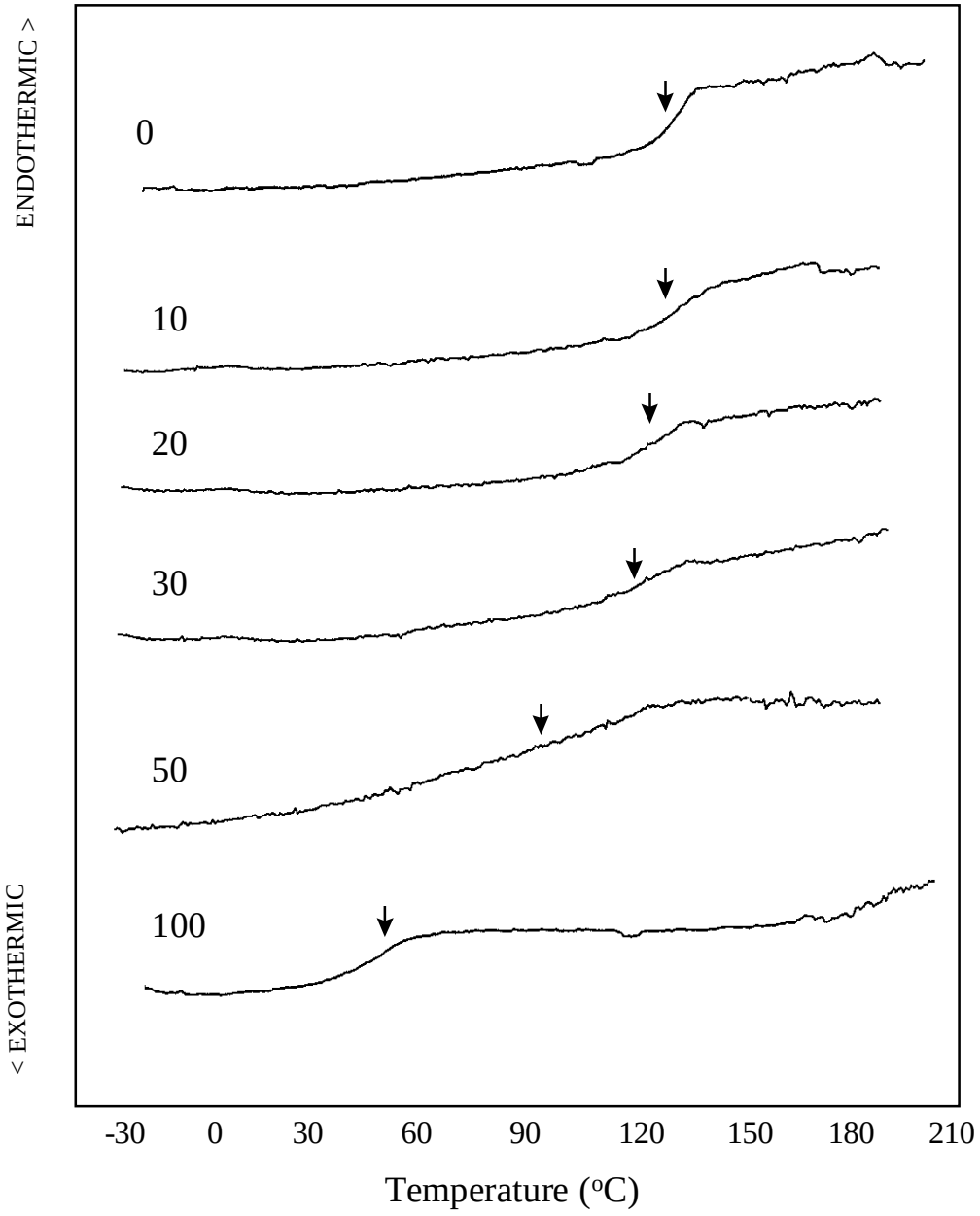

Figure 3.6 : DSC thermograms of solvent ($CHCl_3$) cast samples of CAB and Lignin Hexanoate (LH). Numbers on each curve denote LH content (wt.%) in the blend. These traces are from the second heating scan.

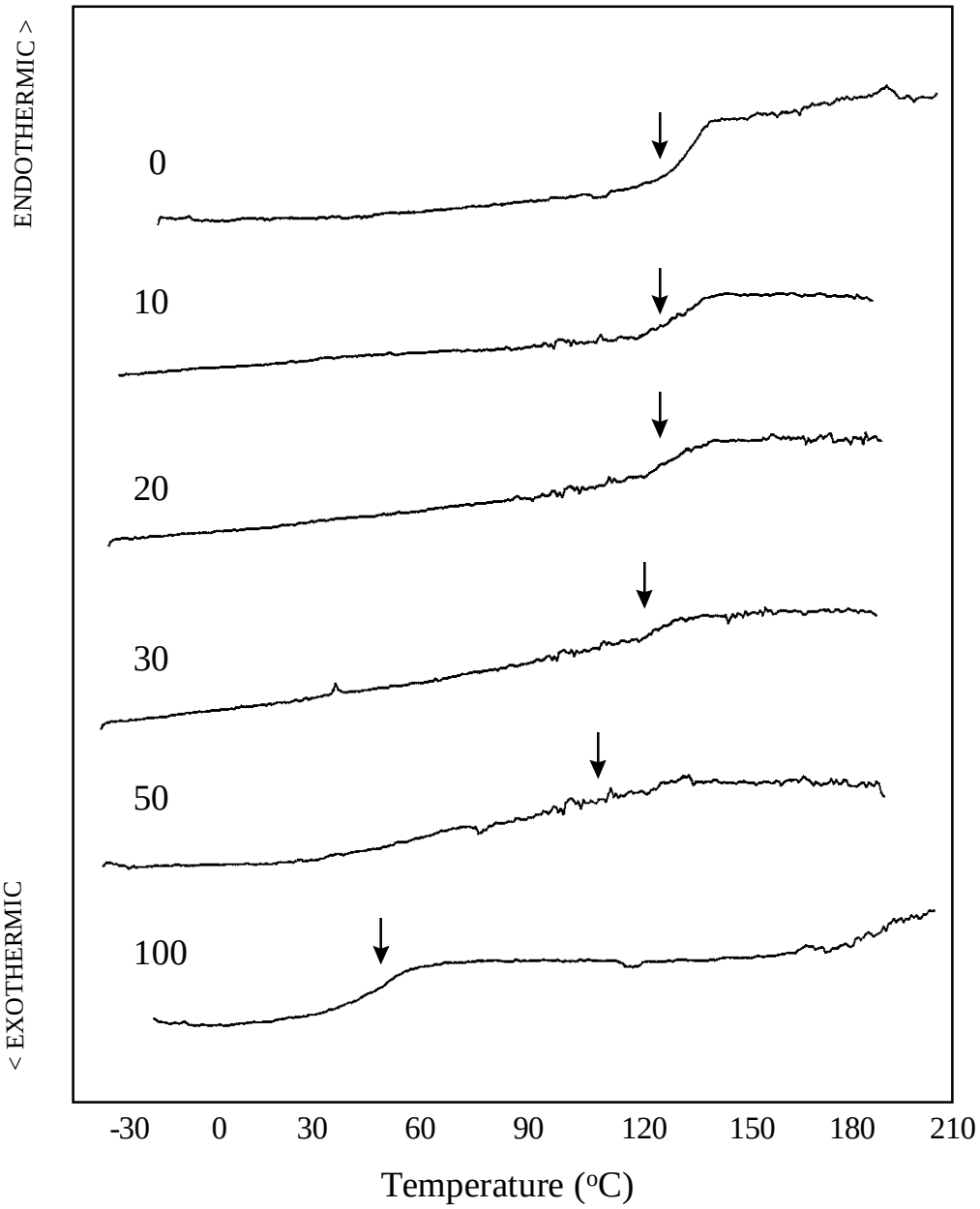

Figure 3.7 : DSC thermograms of melt blended samples of CAB and Lignin Hexanoate (LH). Numbers on each curve denote LH content (wt.%) in the blend. These traces are from the second heating scan.

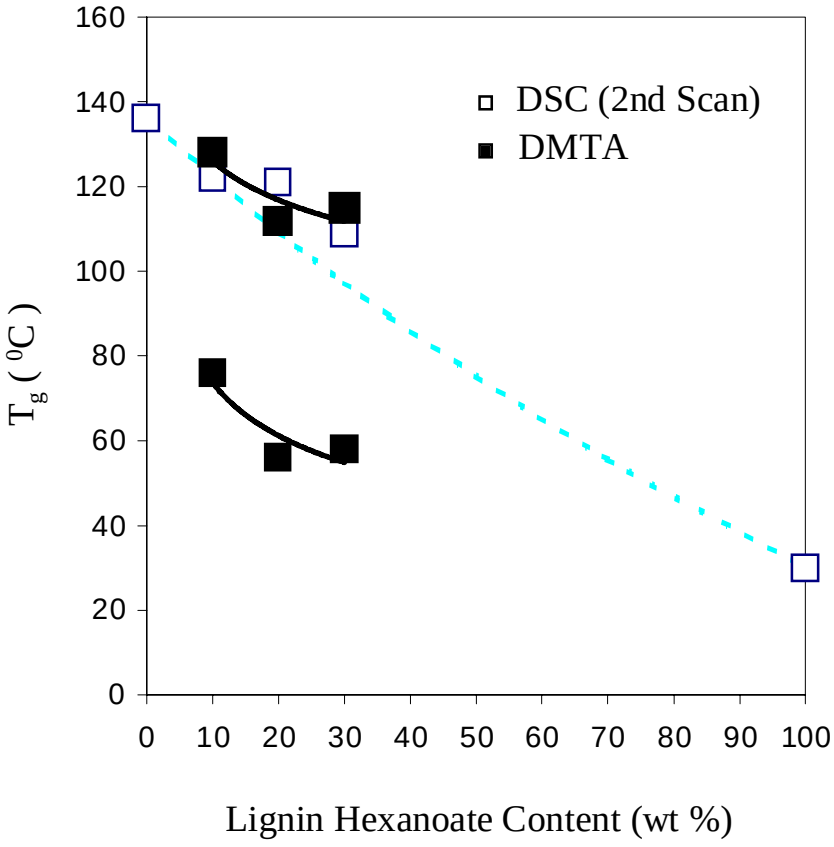

Figure 3.8 : Fox equation fit for blends of CAB and LH.

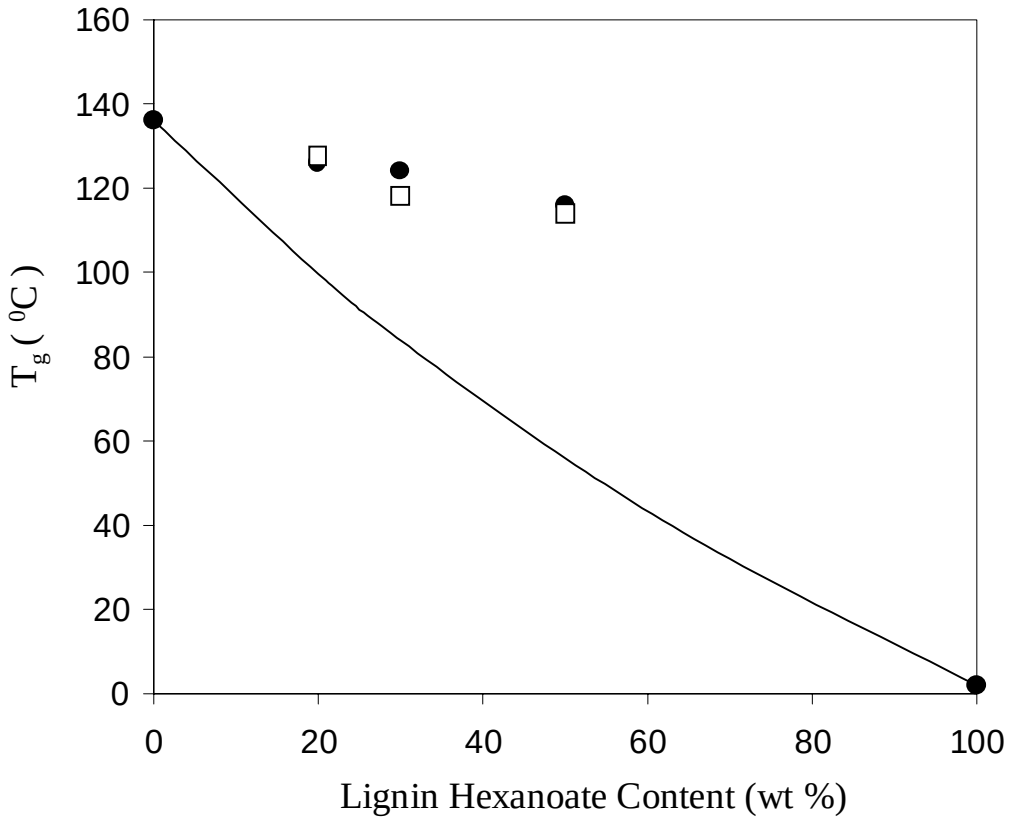

Figure 3.9 : Fox equation fit for blends of CAB and LL.
(■ DSC (2nd Scan), □ DMTA)

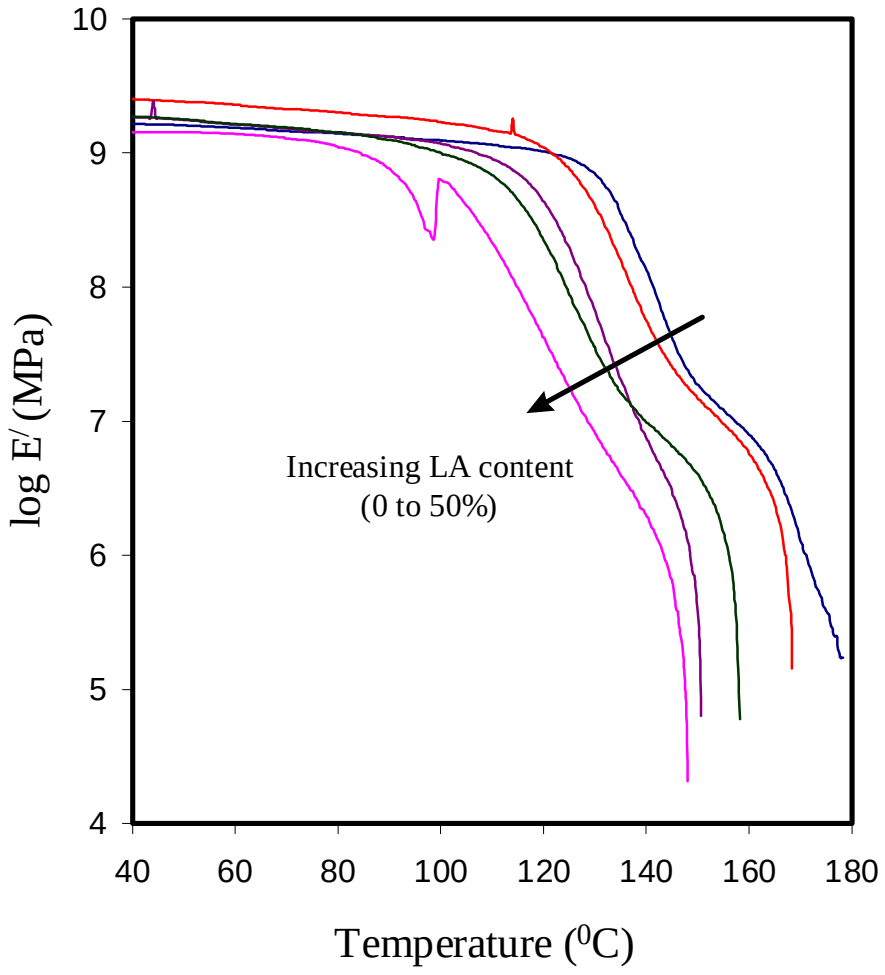

Figure 3.10 : Storage modulus vs. temperature curves for melt blends of CAB and LA obtained from DMTA experiments at 1 Hz in bending mode.

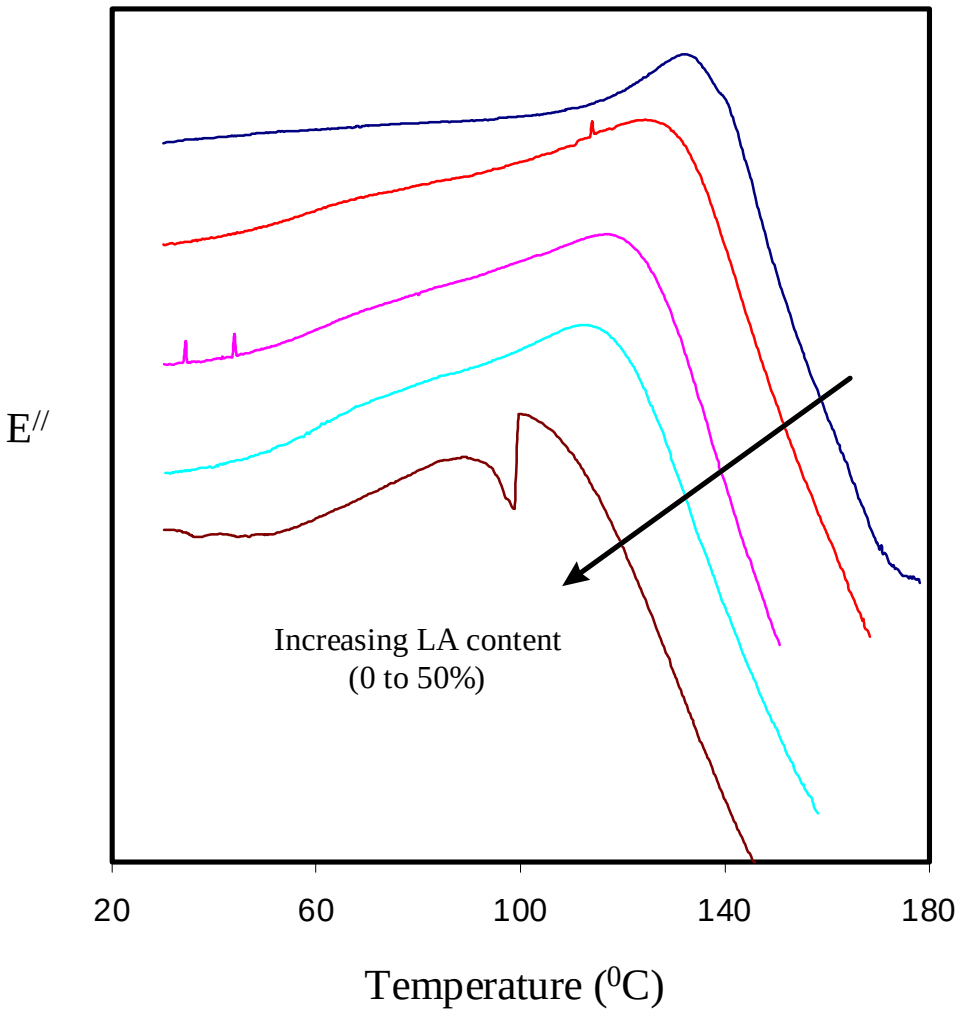

Figure 3.11 : Loss modulus vs. temperature curves for melt blends of CAB and LA obtained from DMTA experiments at 1 Hz in bending mode. Curves have been shifted on the modulus axis for greater clarity.

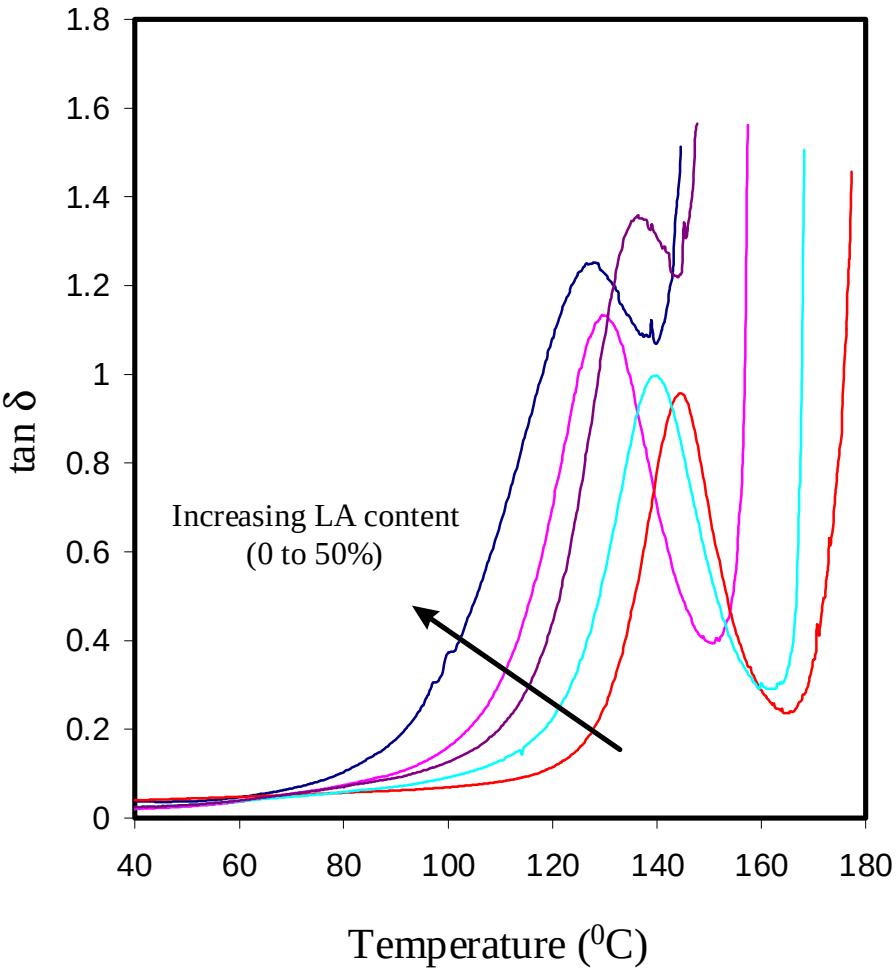

Figure 3.12 : Tan δ vs. temperature curves for melt blends of CAB and LA obtained from DMTA experiments at 1 Hz in bending mode.

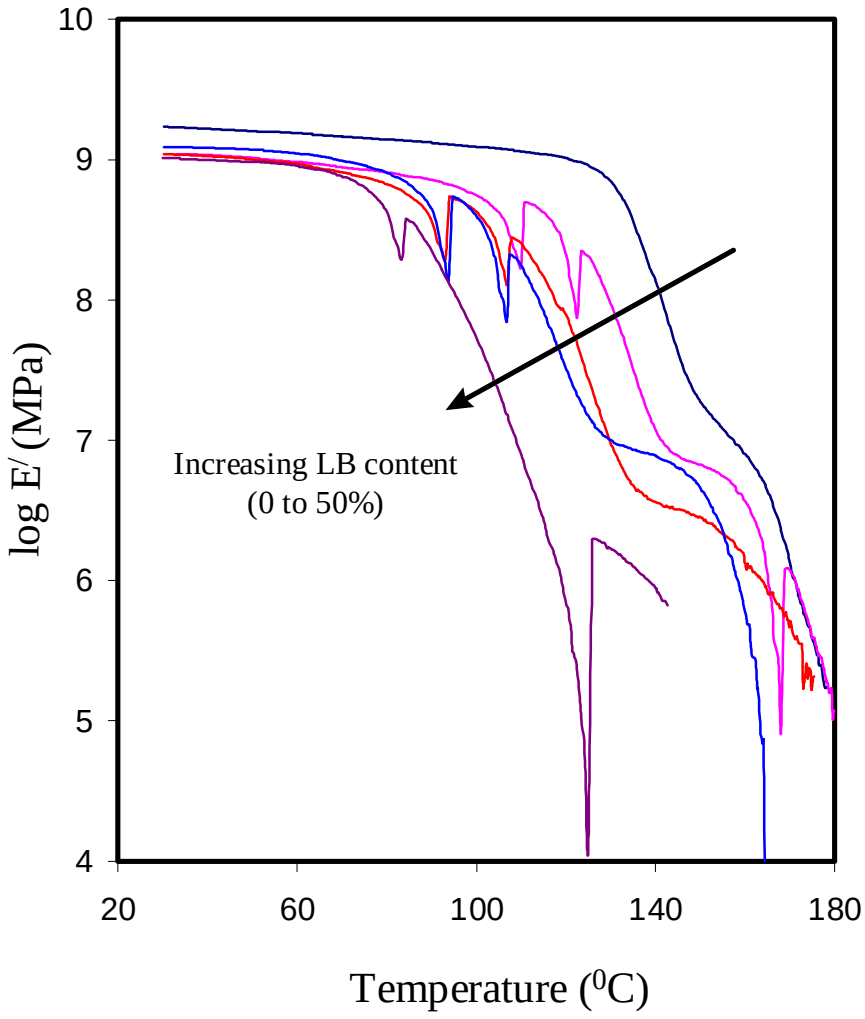

Figure 3.13 : Storage modulus vs. temperature curves for melt blends of CAB and LB obtained from DMTA experiments at 1 Hz bending mode. (Discontinuities in curves are due to thermal expansion effects when the DMTA goes out of balance).

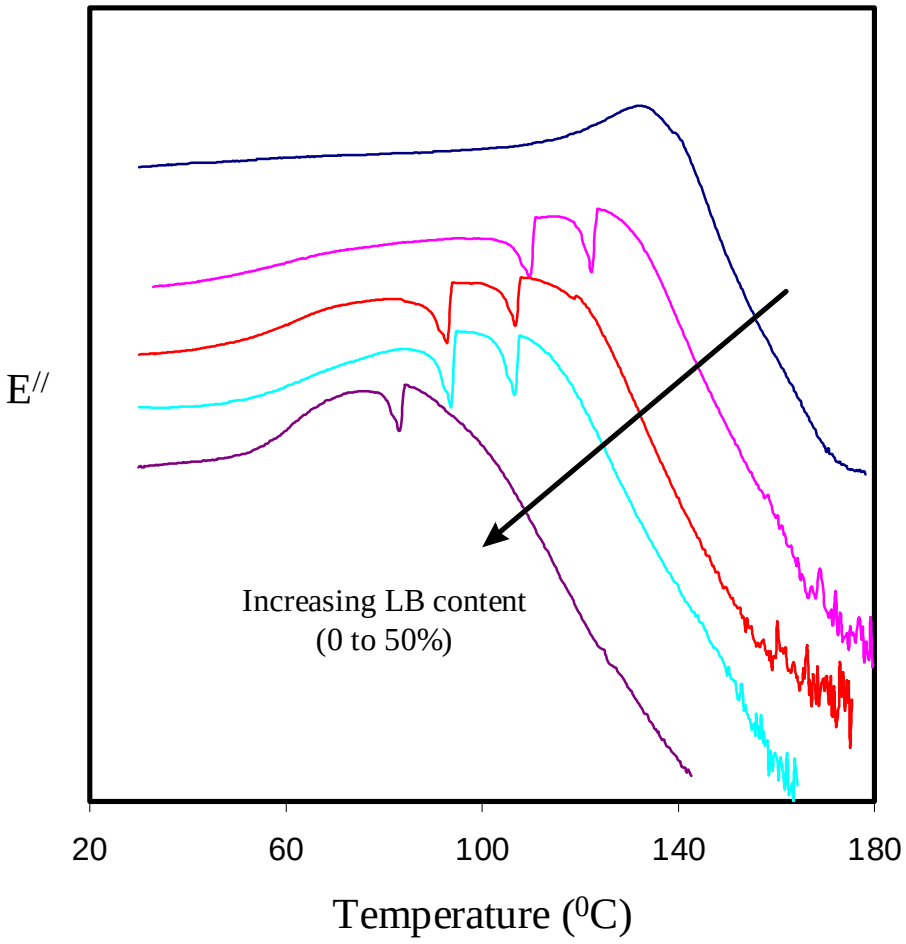

Figure 3.14 : Loss modulus vs. temperature curves for melt blends of CAB and LB obtained from DMTA experiments at 1 Hz in bending mode. Curves have been shifted on the modulus axis for greater clarity.

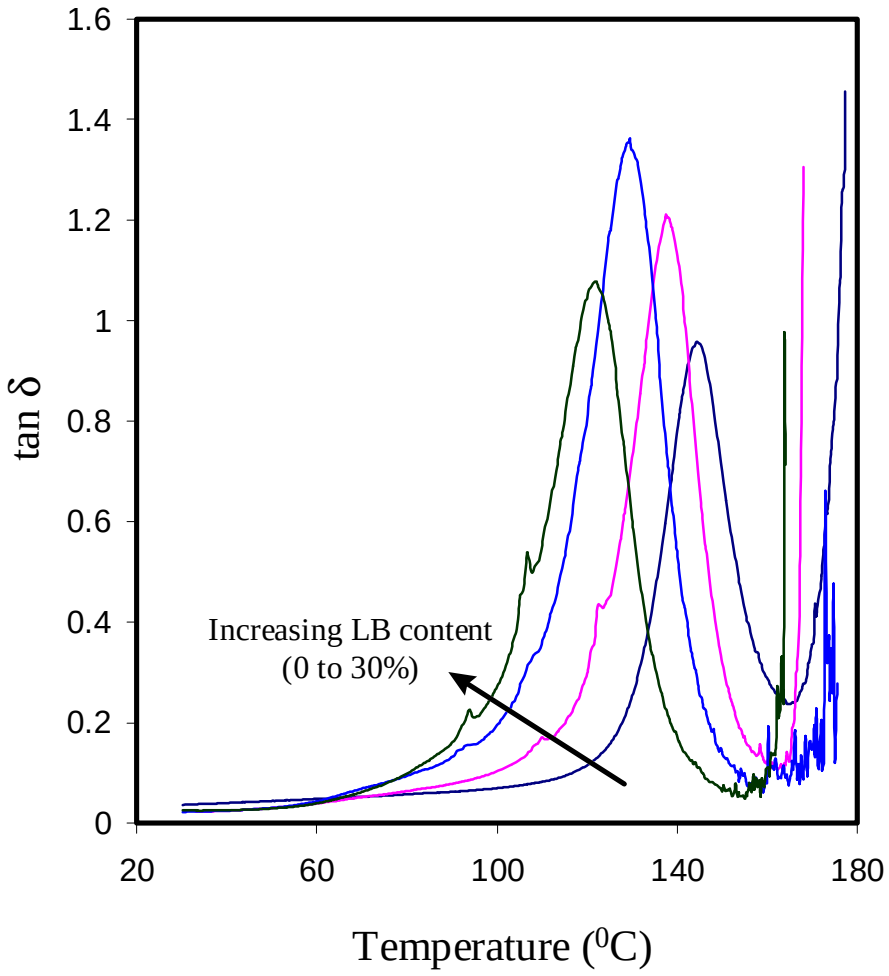

Figure 3.15 : Tan δ vs. temperature curves for melt blends of CAB and LB obtained from DMTA experiments at 1 Hz in bending mode.

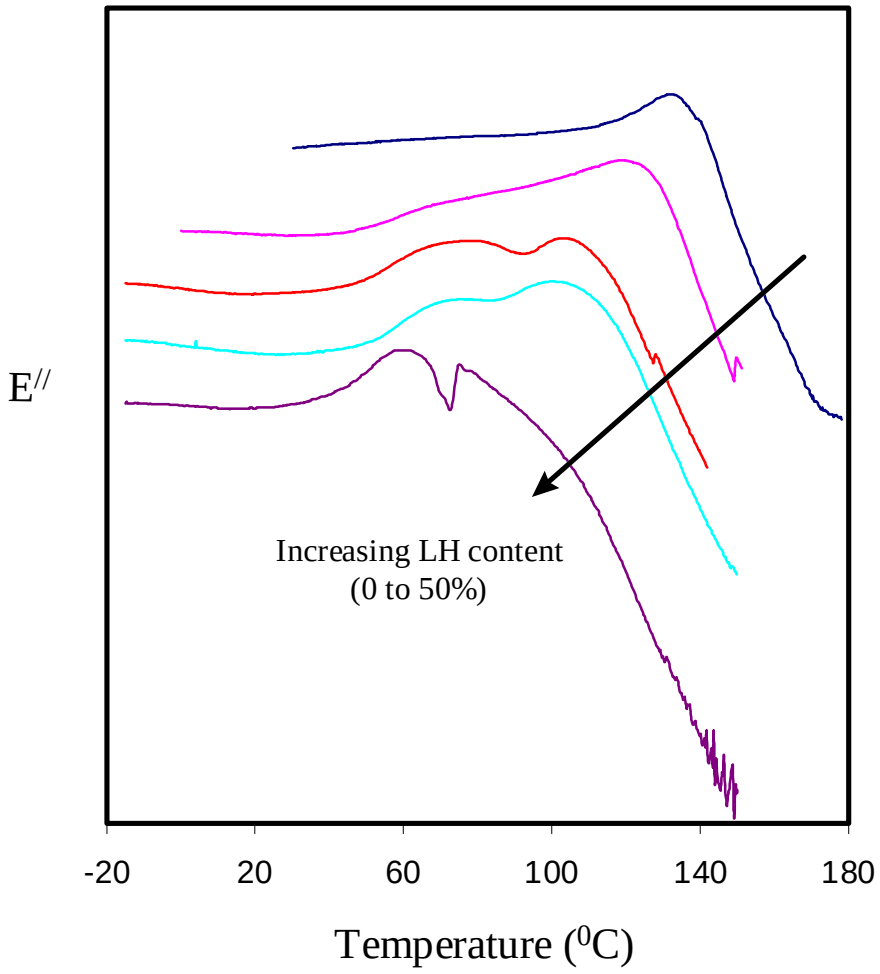

Figure 3.16 : Loss modulus vs. temperature curves for melt blends of CAB and LH obtained from DMTA experiments at 1 Hz in bending mode. Curves have been shifted on the modulus axis for greater clarity.

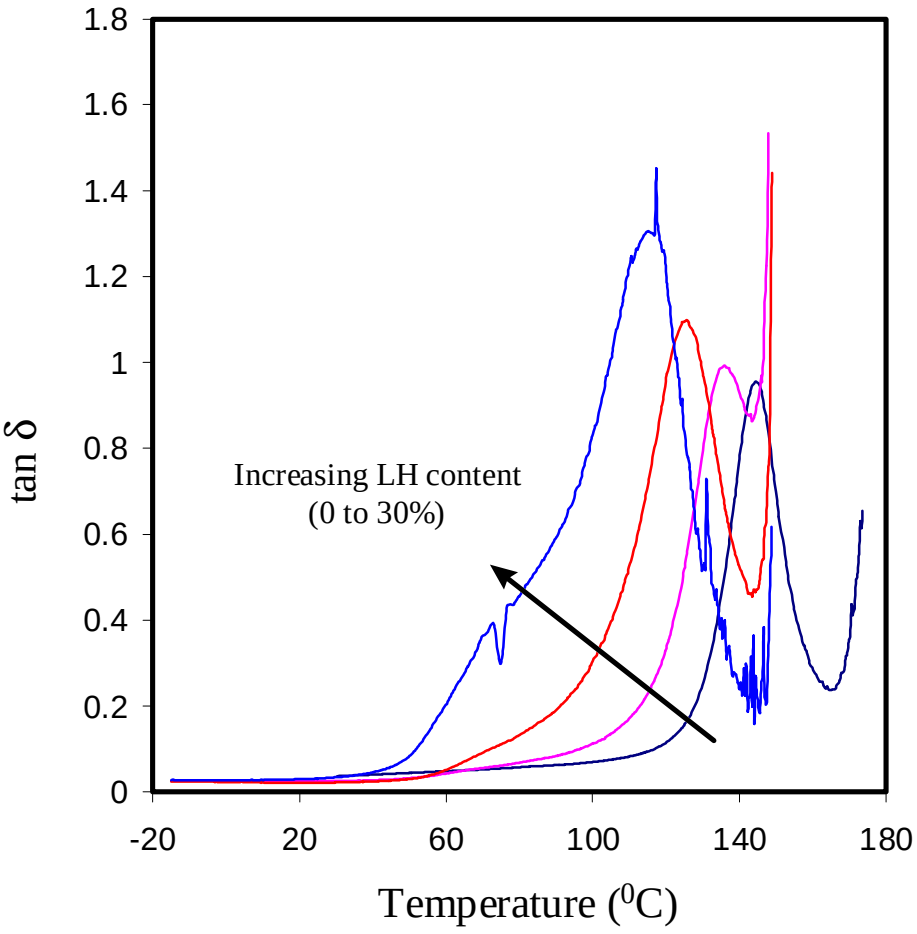

Figure 3.17 : Tan δ vs. temperature curves for melt blends of CAB and LH obtained from DMTA experiments at 1 Hz in bending mode.

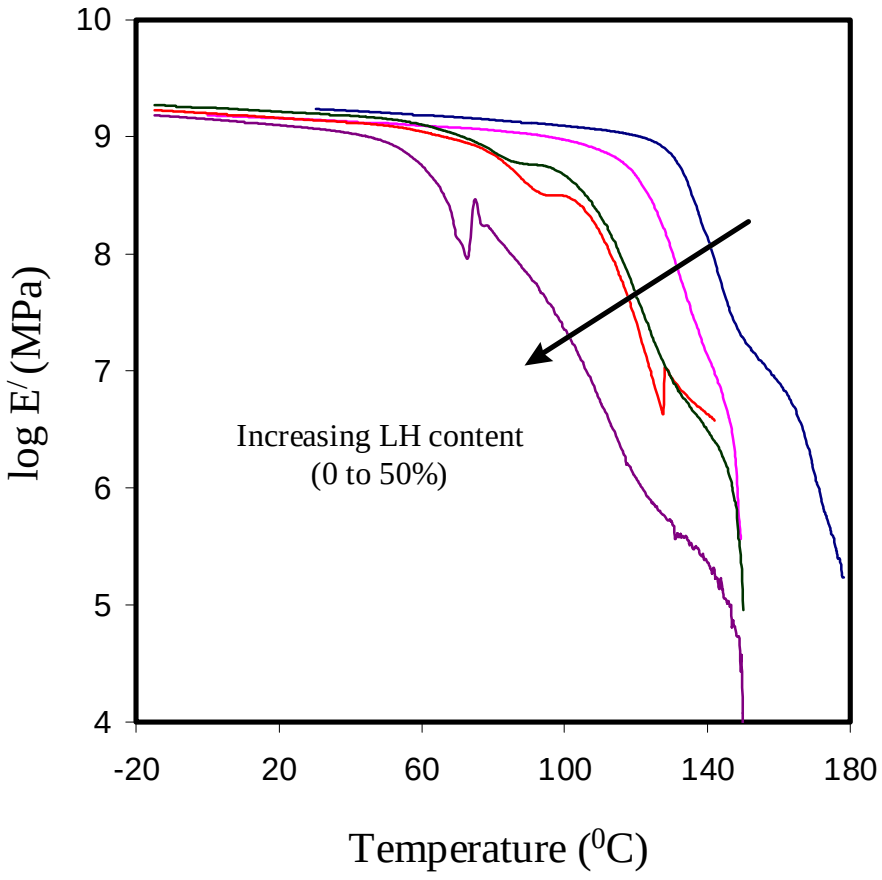

Figure 3.18 : Storage modulus vs. temperature curves for melt blends of CAB and LH obtained from DMTA experiments at 1 Hz in bending mode.

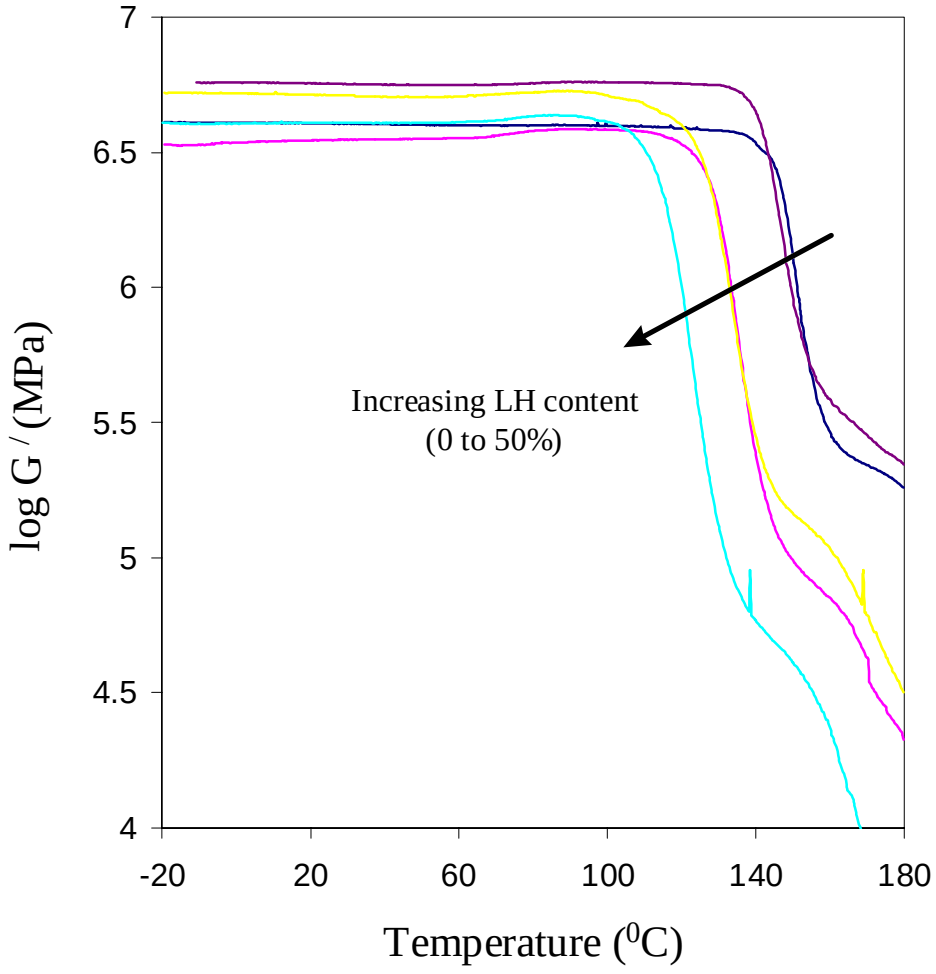

Figure 3.19 : Storage modulus vs. temperature curves for solvent cast blends of CAB and LH obtained from DMTA experiments at 1 Hz in shear mode.

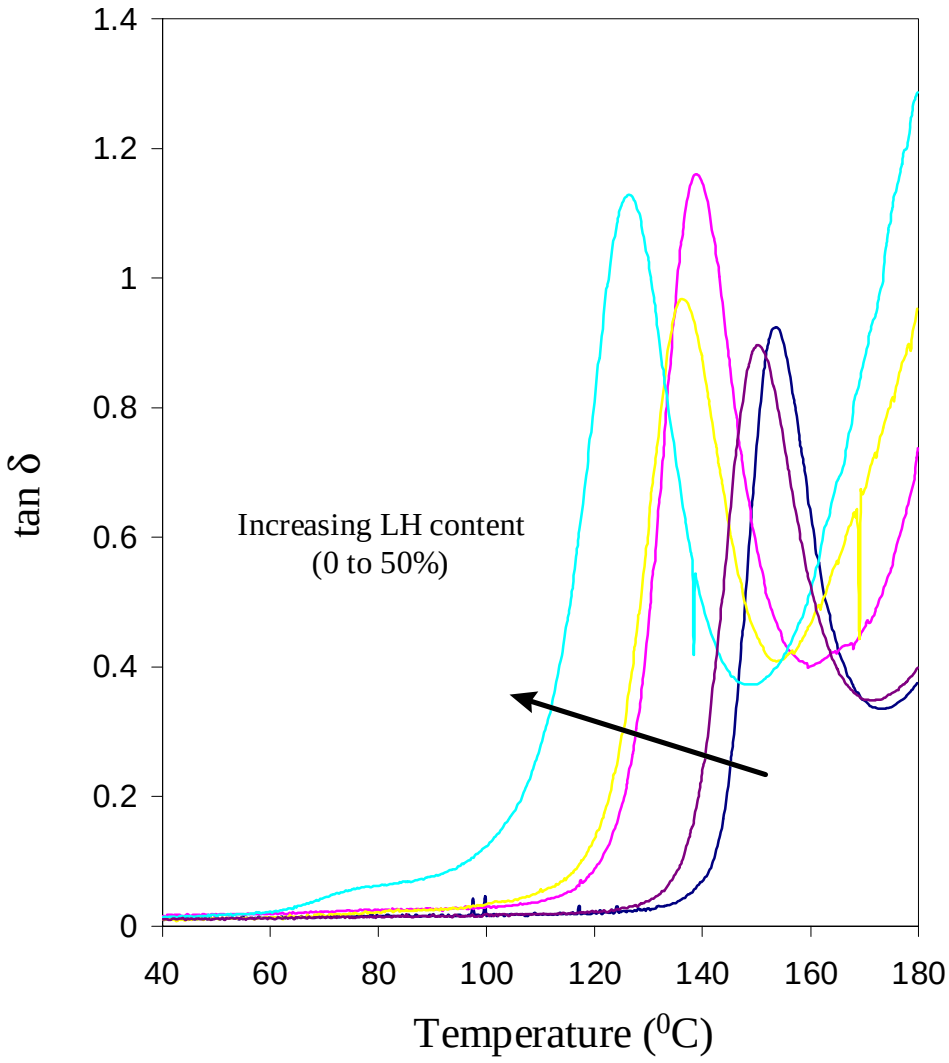

Figure 3.20 : Tan δ vs. temperature curves for solvent cast blends of CAB and LH obtained from DMTA experiments at 1 Hz in shear mode.

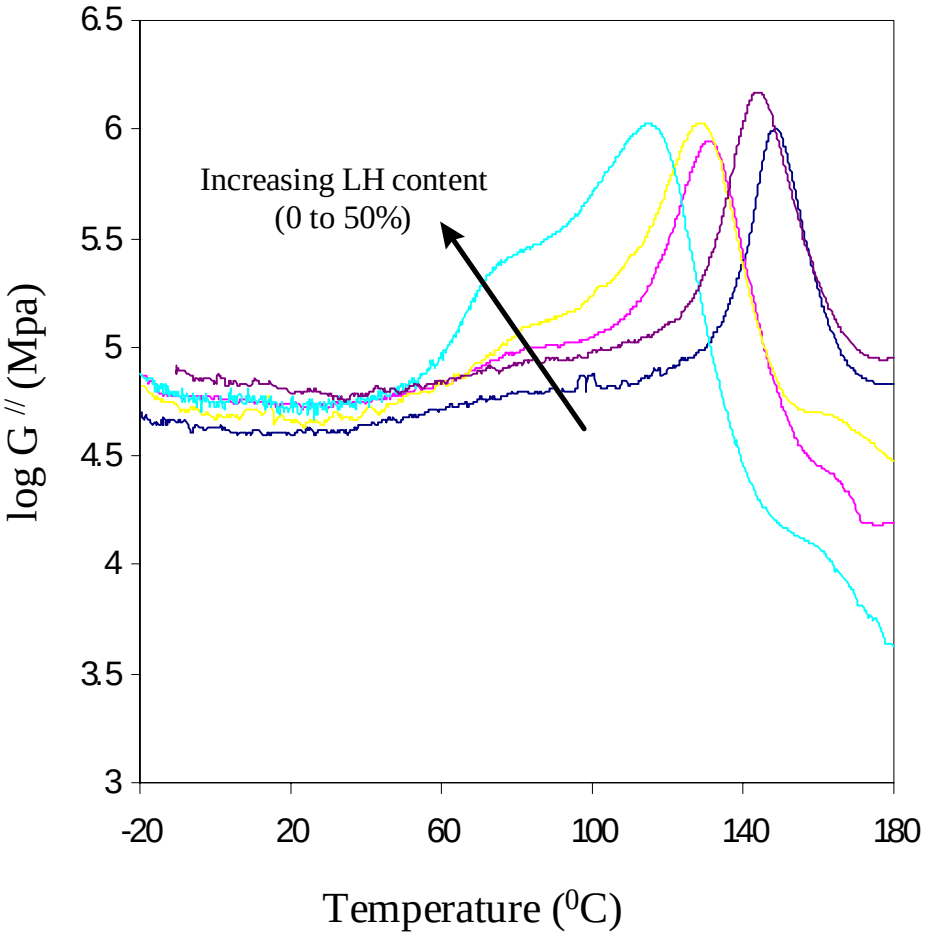

Figure 3.21 : Loss modulus vs. temperature curves for solvent cast blends of CAB and LH obtained from DMTA experiments at 1 Hz in shear mode.

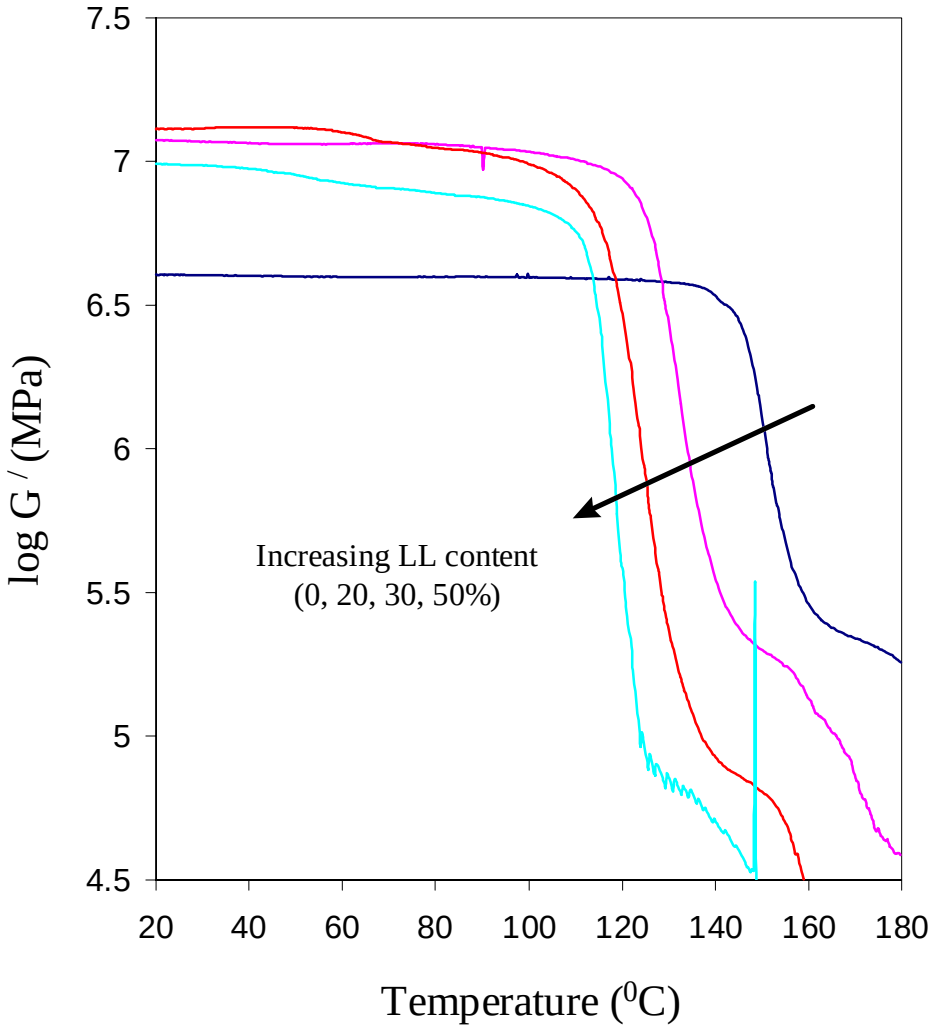

Figure 3.22 : Storage modulus vs. temperature curves for solvent cast blends of CAB and LL obtained from DMTA experiments at 1 Hz in shear mode.

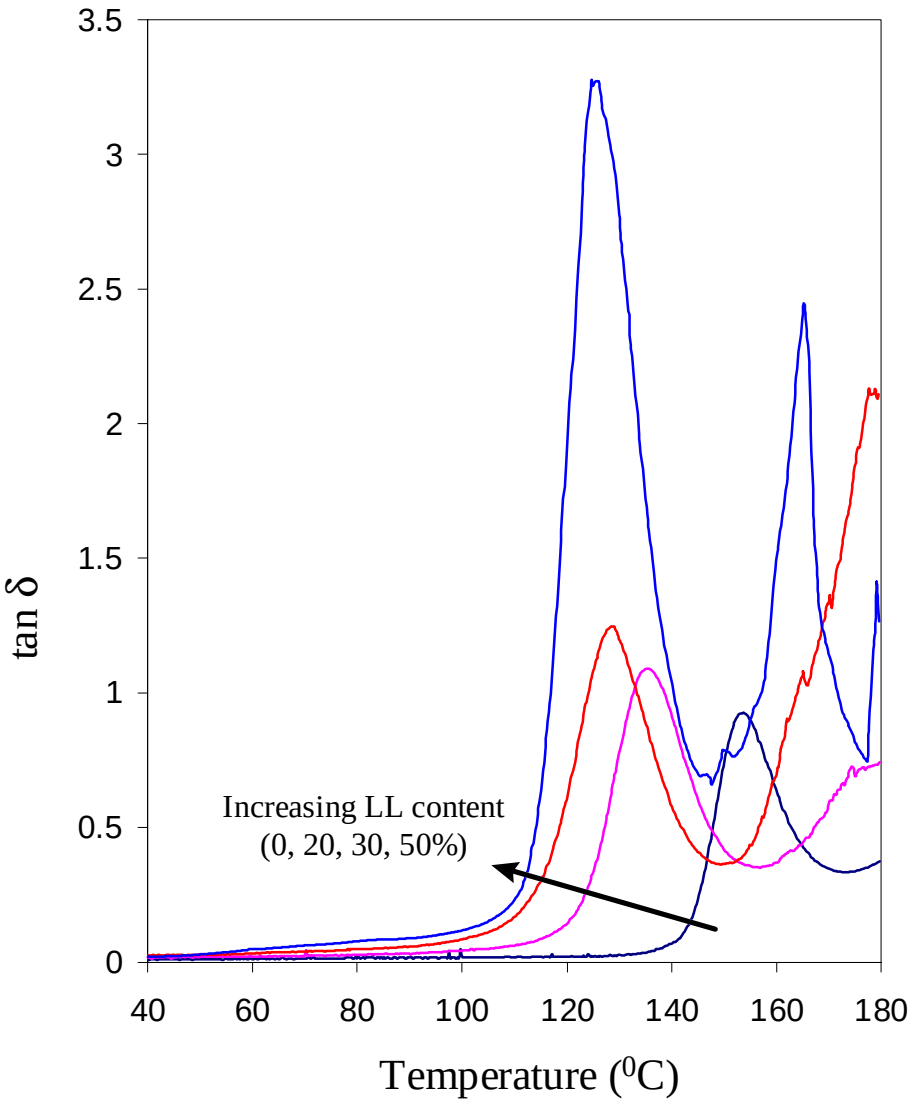

Figure 3.23 : Tan δ vs. temperature curves for solvent cast blends of CAB and LL obtained from DMTA experiments at 1 Hz in shear mode.

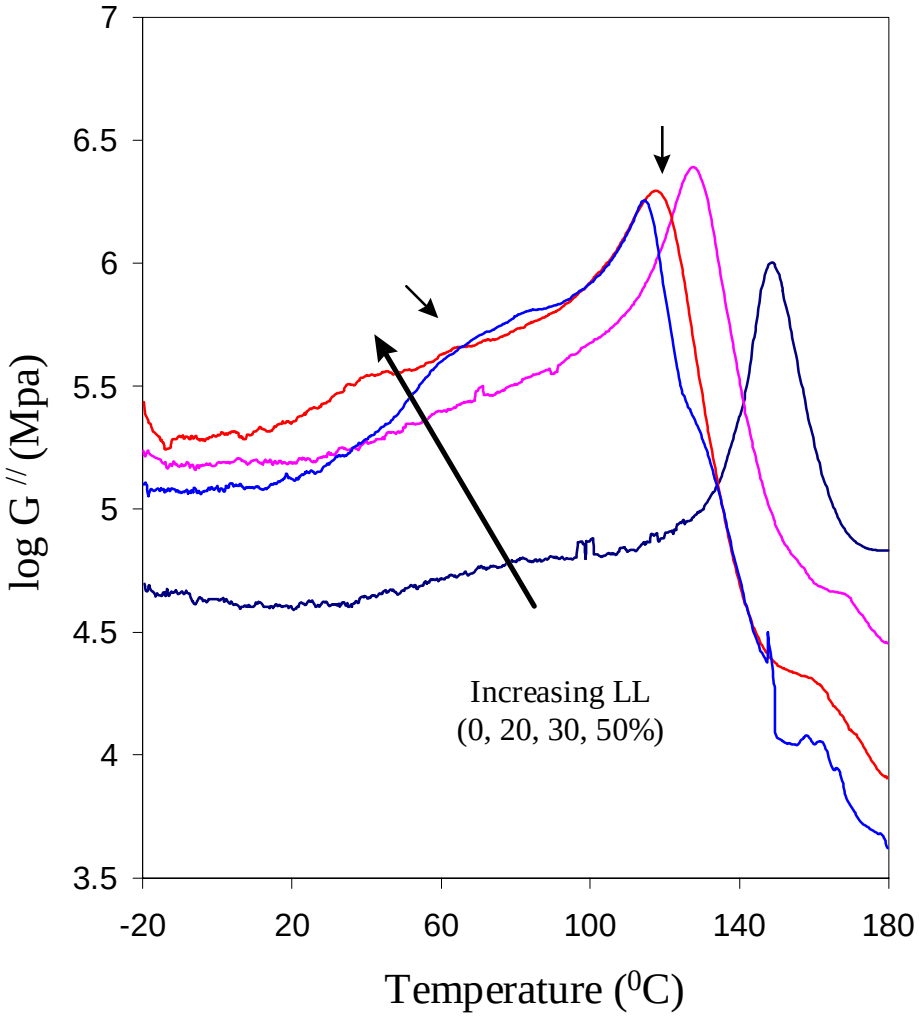

Figure 3.24 : Loss modulus vs. temperature curves for solvent cast blends of CAB and LL obtained from DMTA experiments at 1 Hz in shear mode.

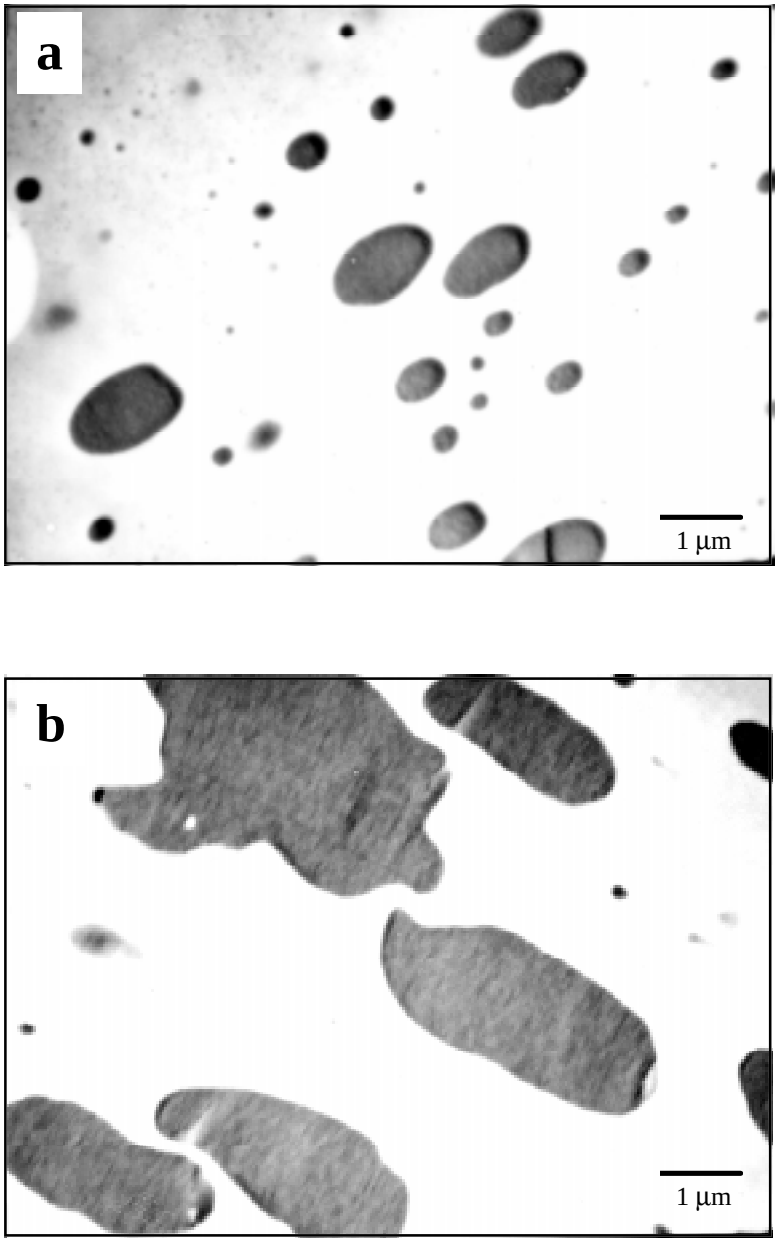

Figure 3.25 : Transmission electron micrographs of solvent cast samples of CAB blends with (a) 20% LH and (b) 50% LH content by weight (magnification at 10,000 X).

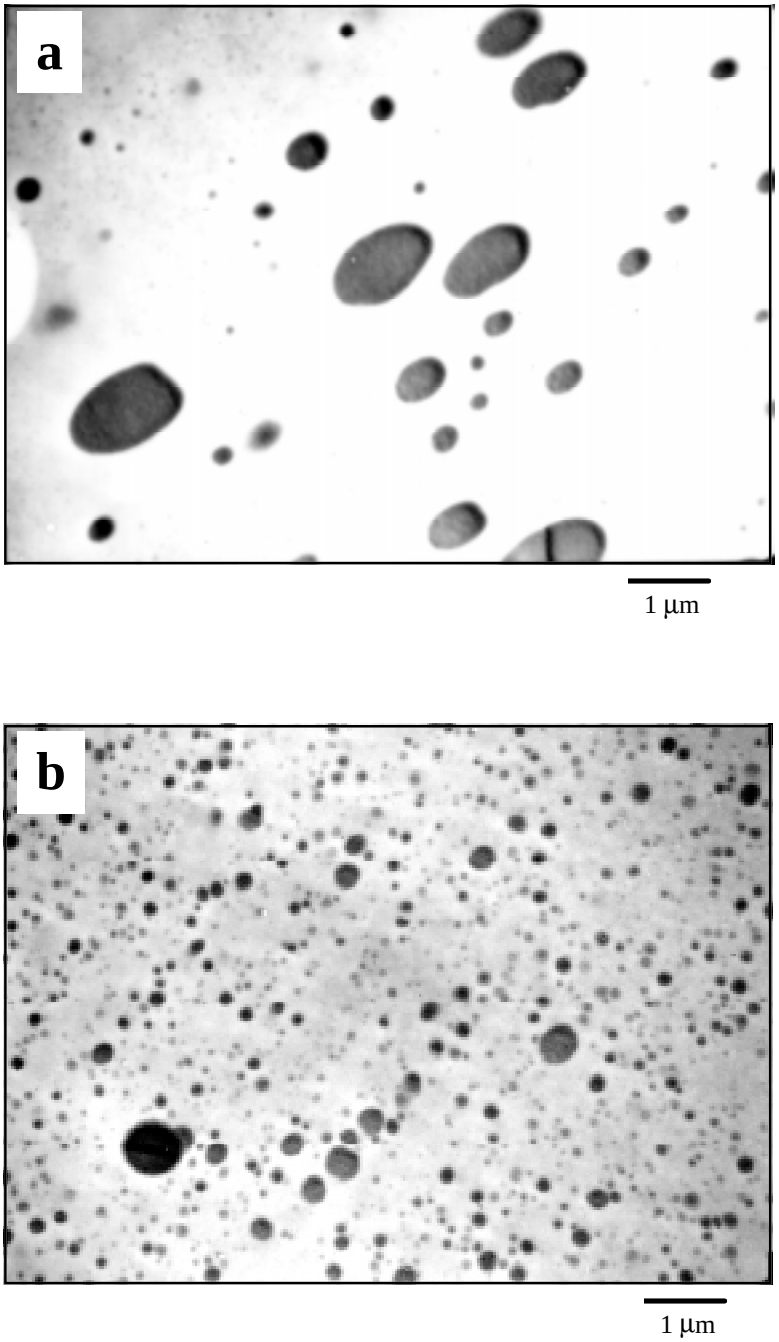

Figure 3.26 : Transmission electron micrographs of (a) solvent cast and (b) melt blended samples of CAB with 20% LH by weight (magnification at 10,000 X).

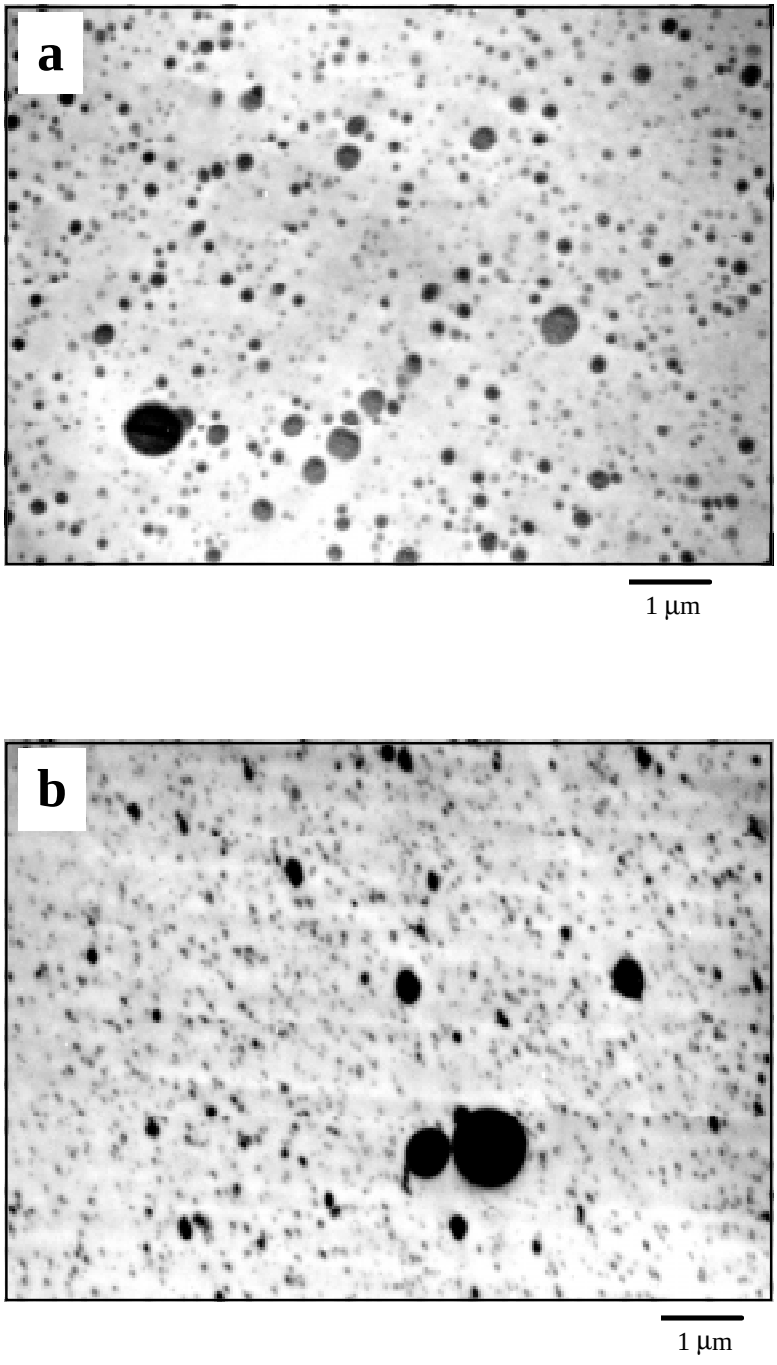

Figure 3.27 : Transmission electron micrographs of melt blended samples CAB with (a) 20% LH and (b) 20% LA content by weight (magnification at 10,000 X).

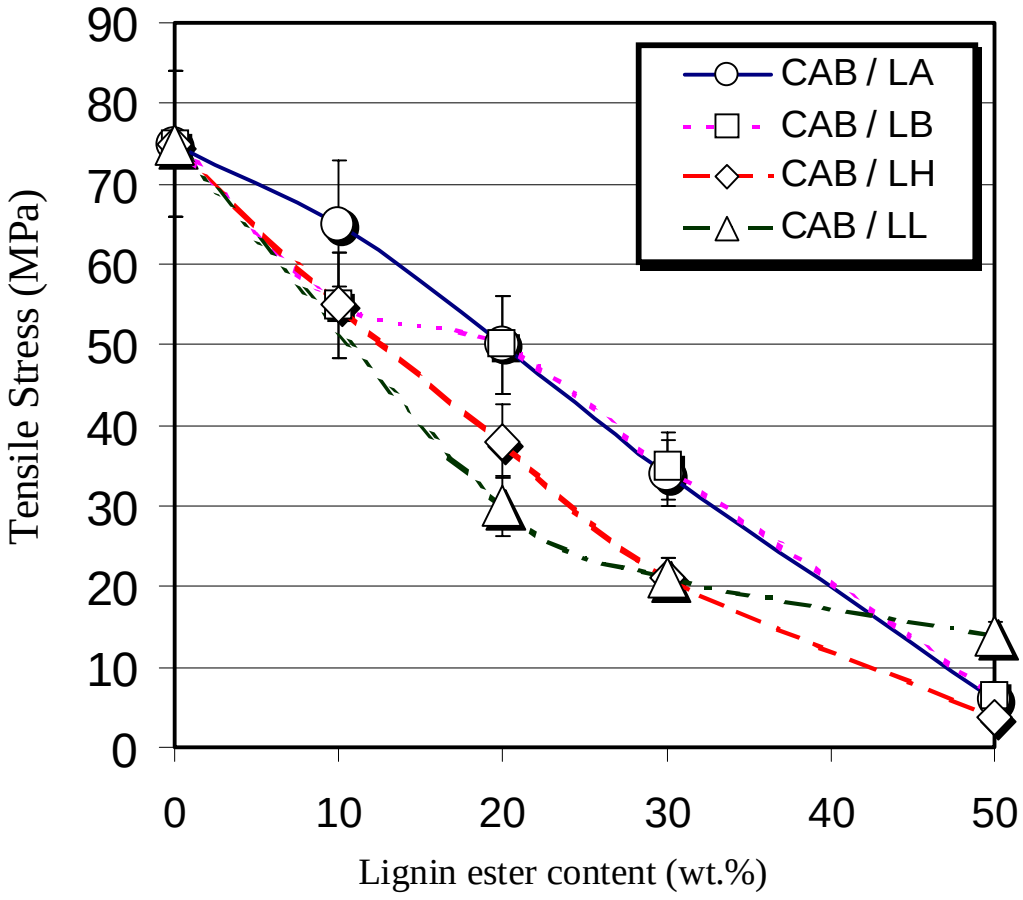

Figure 3.28 : Tensile stress vs. lignin ester content for CAB/lignin ester blends.

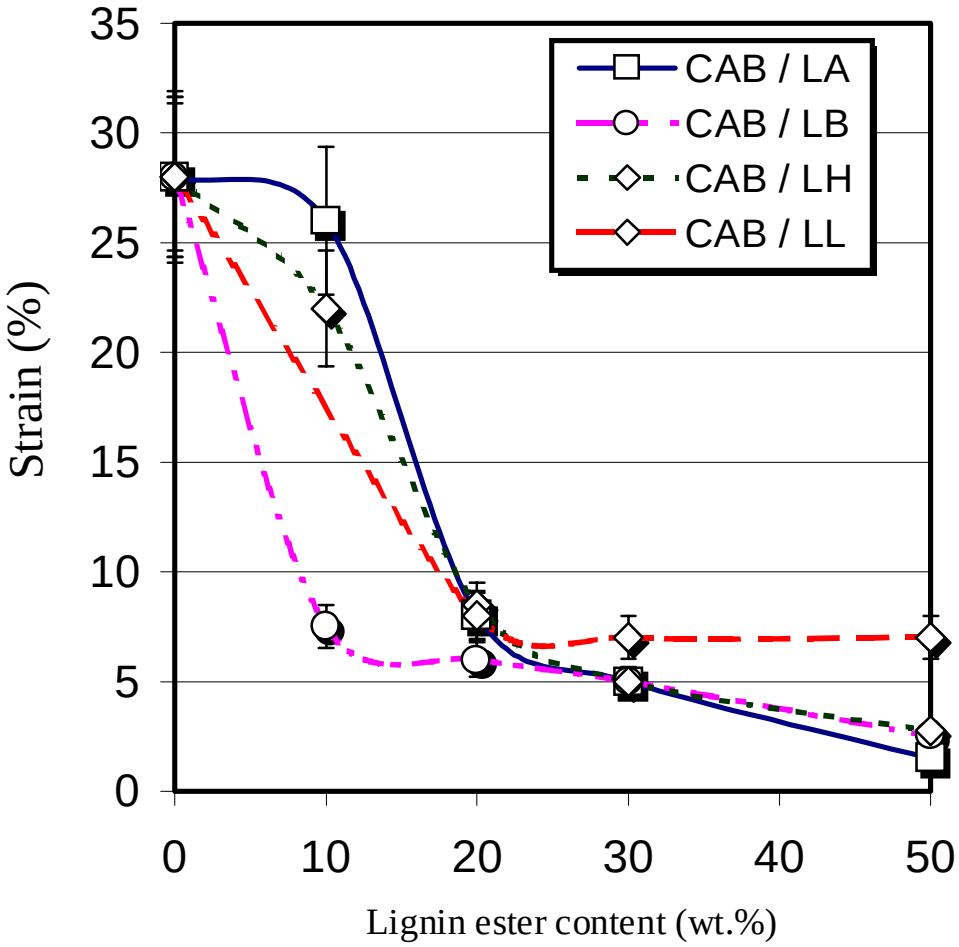

Figure 3.29 : Strain (at break) vs. lignin ester content for melt blended samples of CAB/lignin ester.

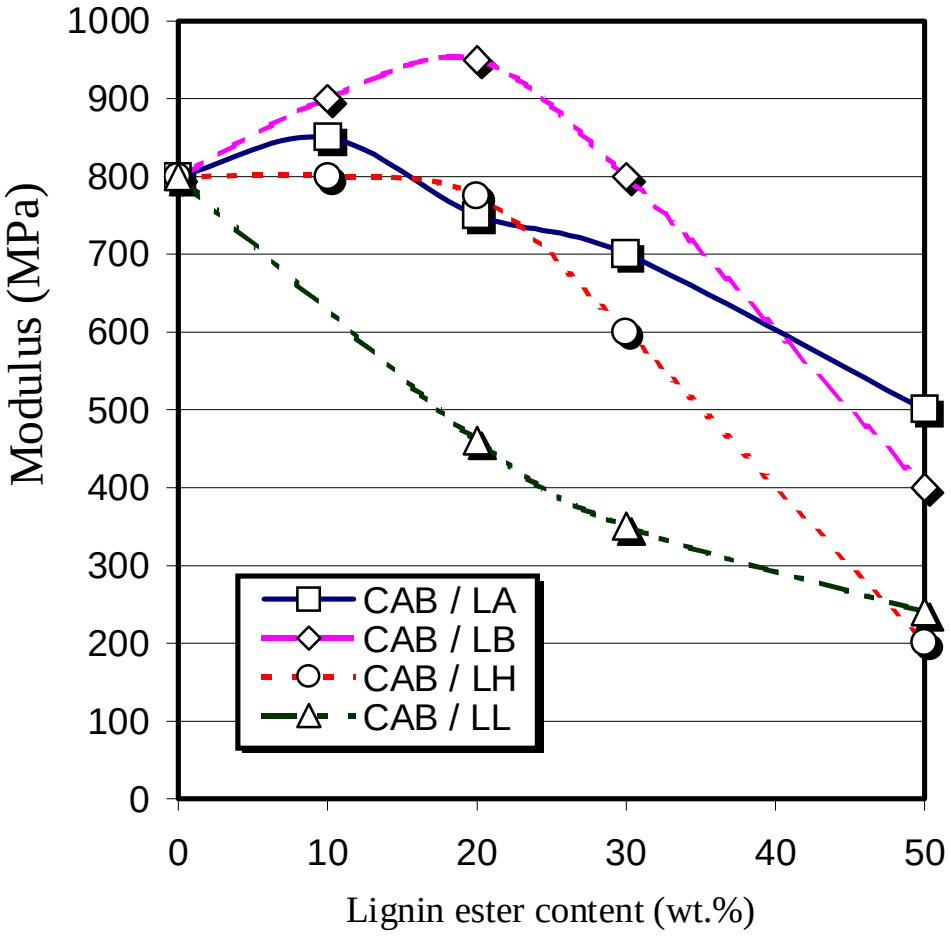

Figure 3.30 : Modulus vs. lignin ester content for melt blended samples of CAB/lignin ester.

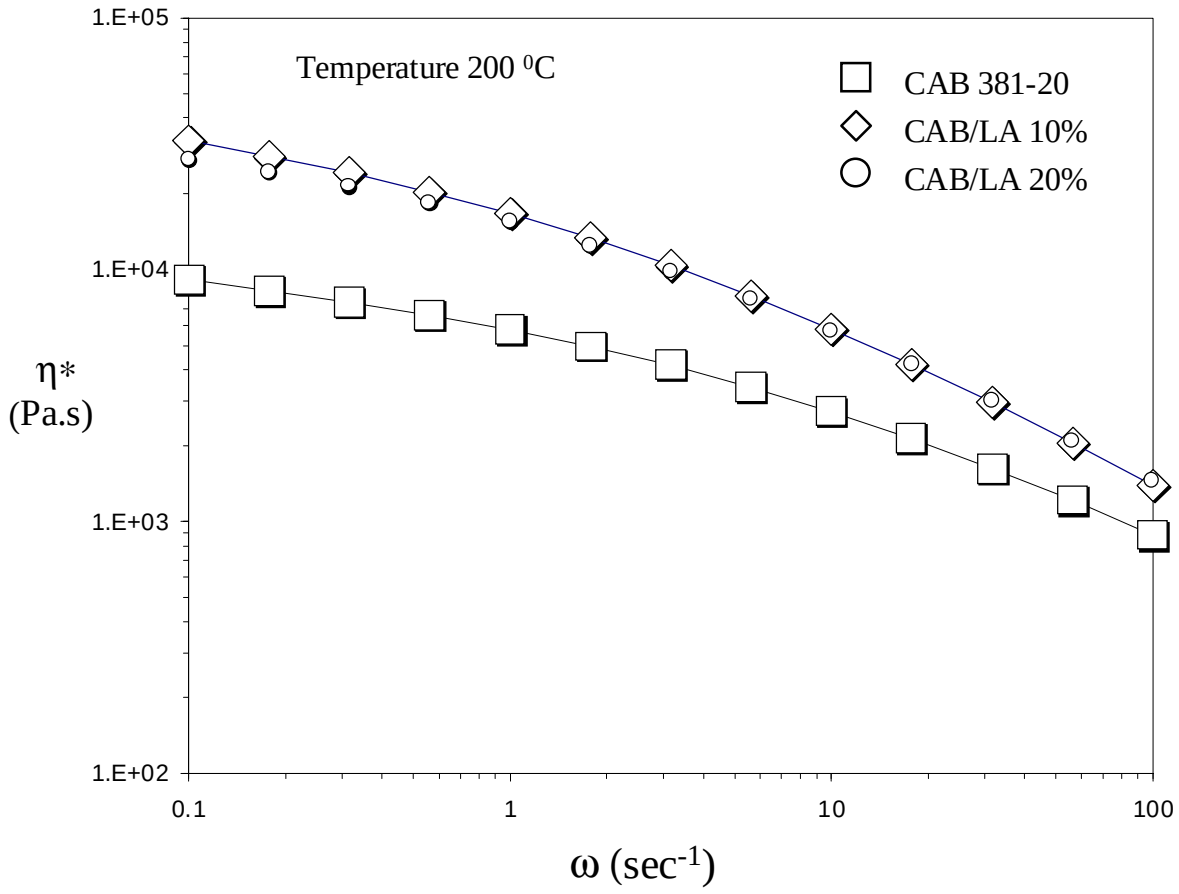

Fig. 3.31 : Viscosity data for different blends of CAB/LA at 200 ^{0}C.

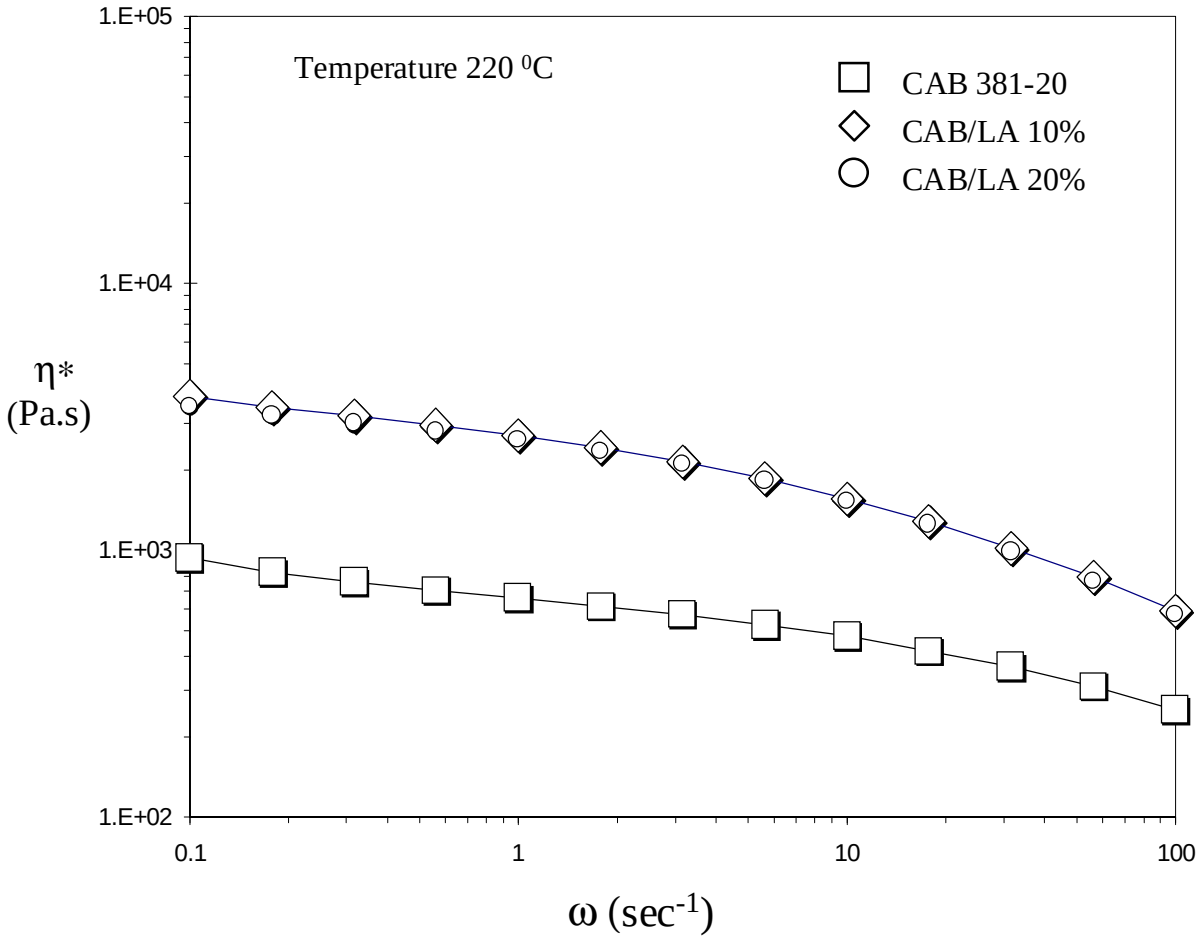

Fig. 3.32 : Viscosity data for different blends of CAB/LA at 220 ^{0}C.

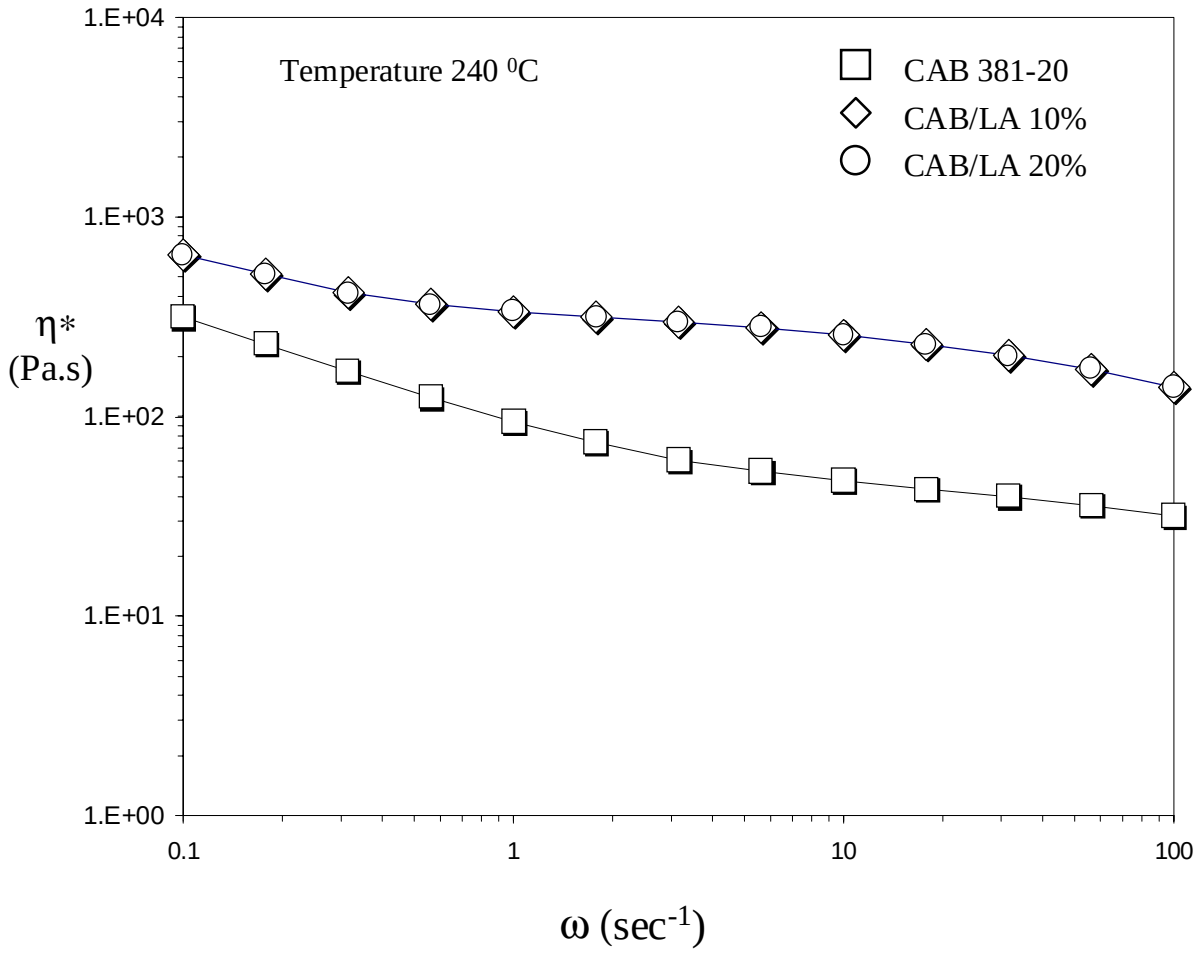

Fig. 3.33 : Viscosity data for different blends of CAB/LA at 240 ^{0}C.

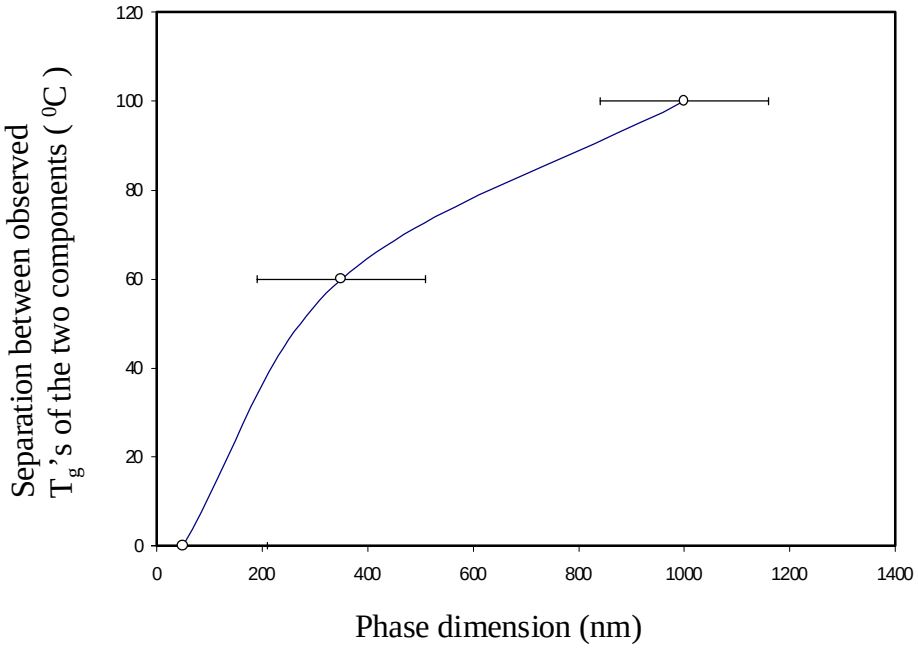

Figure 3.34 : Comparison between the dimensions of the lignin ester phases and the corresponding difference in the observed glass transtion relaxations of CAB and Lignin esters blends.